~~S. C. DUNN~~

[redacted]

AEDC-TR-71-60

[redacted]

ANALYTICAL MODEL OF AN EXHAUST GAS COOLING SYSTEM EMPLOYING LIQUID INJECTION

J. M. Pelton and C. E. Willbanks

ARO, Inc.

June 1971

[redacted]

Approved for public release; distribution unlimited.

ENGINE TEST FACILITY

ARNOLD ENGINEERING DEVELOPMENT CENTER

AIR FORCE SYSTEMS COMMAND

ARNOLD AIR FORCE STATION, TENNESSEE

NOTICES

ANALYTICAL MODEL OF AN EXHAUST GAS COOLING SYSTEM EMPLOYING LIQUID INJECTION

J. M. Pelton and C. E. Willbanks
ARO, Inc.

FOREWORD

The work reported herein was conducted at the request of the Arnold Engineering Development Center (AEDC), Air Force Systems Command (AFSC), Arnold Air Force Station, Tennessee, under Annex No. AF-66-G-7406 to the Mutual Weapons Development Plan Master Data Exchange Agreement between the governments of the United States and the Federal Republic of Germany under Program Element 6540223F.

The work involved analytical study and experimental testing conducted by ARO, Inc. (a subsidiary of Sverdrup & Parcel and Associates, Inc.), contract operator of the Arnold Engineering Development Center under Contract F40600-71-C-0002. The cooler test data were taken from tests conducted in the Propulsion Development Test Cell (T-1) spray cooler of the Engine Test Facility (ETF) under ARO Project No. RW0856, and the manuscript was submitted for publication on October 28, 1970.

Grateful acknowledgment is made to J. M. Rose and W. C. Moger of the Scientific Computing Center for assistance in programming the IBM 360 computer. Acknowledgment is also made to C. E. Peters, ETF Special Projects Branch; H. K. Clark and R. A. Thompson, ETF Facility Support Branch; and P. J. Bohn, University of Tennessee Space Institute Research Assistant, for their valuable contributions to the technical program.

This technical report has been reviewed and is approved.

Donald E. Beitsch
Lt Colonel USAF
Operations Division
Directorate of Test

Joseph R. Henry
Colonel, USAF
Director of Test

ABSTRACT

An analysis was undertaken to better understand the phenomena occurring in spray coolers and to develop a mathematical model for comparison with experimental data from an operating unit. The physical characteristics of an operational exhaust gas spray cooler and the instrumentation systems are described. A mathematical model of a spray cooler was developed by assuming kinetic and thermodynamic equilibrium and one-dimensional flow. A mathematical model of a hypothetical, optimum cooler is included in order to have a basis for defining cooler efficiency. The equations were programmed for numerical solution on a digital computer, and several trial case runs are presented. Experimental measurements are compared with the efficiencies predicted by the mathematical models.

CONTENTS

APPENDIXES

I. ILLUSTRATIONS

NOMENCLATURE

A	Cross-sectional area, ft^2
a, b, c	Quadratic equation coefficient
c_p	Specific heat at constant pressure, Btu/lbm °R
F	Ratio of masses, $\dot{m}_{w_1}/\dot{m}_{nc}$
G1...G8	Influence coefficients defined in Figs. III-1b and c
g_c	Gravitational constant, lbm ft/lbf sec^2
h	Enthalpy, Btu/lbm
$\dot{m}$	Mass flow rate, lbm/sec
$\bar{m}$	Molecular weight, lbm/lbm-mole
P	Pressure, lbf/ft^2
$\dot{Q}$	Volumetric flow rate, ft^3/sec
q	Dynamic pressure, lbf/ft^2
R	Gas constant, lbf ft/lbm °R
$\bar{R}$	Universal gas constant, lbf ft/lbm-mole °R
T	Temperature, °R
V	Velocity, ft/sec
X	Coefficient
Δ	Incremental change
η	Efficiency
ρ	Mass density, lbm/ft^3

SUBSCRIPTS

1	Inlet (evaporation section)
2	Exit (evaporation section), Inlet (dehumidification section)
3	Exit (dehumidification section)
D	Drain
fg	Change by evaporation
nc	Noncondensable
s	Saturation
v	Vapor
w	Water

SECTION I
INTRODUCTION

Testing of turbojet engines and rocket motors at simulated altitude in ground test facilities requires cooling of the high temperature exhaust gas to a relatively low temperature before the gas enters the exhaust gas pumping system. Cooling of the gases by water spray with direct heat and mass exchange between the water and the exhaust gas has been utilized in many test facilities. This method of cooling is often called spray cooling.

Many of the spray coolers used in the Engine Test Facility (ETF) at the Arnold Engineering Development Center (AEDC) receive exhaust gas from a rocket or turbojet engine. The cooling process reduces the temperature from approximately 4000°R (maximum temperature of a turbojet engine exhaust gas) to approximately 550°R. By means of an atomizing water spray, the exhaust gas is cooled and dehumidified. The cooling produces a temperature compatible with the ducting, control valves, and pumping system material limits, and the dehumidification maximizes the exhaust gas handling capacity of the exhaust pumping machinery. Water conservation is an important consideration in operation because of the large quantities of spray water required.

There is limited knowledge of the detailed performance of exhaust gas coolers in general and, in particular, of coolers operating at low pressures and with high velocity gas streams. Therefore, a program was initiated with two objectives: (1) to develop a mathematical model to assist in the formulation of design criteria for future coolers, and (2) to define and understand the general operating characteristics of the coolers in use at the ETF. When data collected during exhaust gas cooler operation in support of normal engine test programs are compared with data from the mathematical model, the limits of operation for the coolers currently in use can be determined.

The overall work is being carried out as a joint effort between the Arnold Engineering Development Center (AEDC) and the German Agency for Aeronautics and Space Research (DFVLR). The work at AEDC was conducted in the Engine Test Facility. The cooler performance data were obtained from one of the propulsion engine test cells during actual test runs. Instrumentation for the cooler performance data was installed in the exhaust gas cooler and associated ducting. The work at DFVLR (Refs. 1 and 2) was performed at the Institute for Chemical Rocket Testing at Lampoldshausen. The DFVLR work is developed for low velocity, low mass flow rates of exhaust gas, whereas the work in

ETF is primarily concerned with high velocity, high mass flow rates of exhaust gas.

This report contains the derivation of a mathematical model based on thermodynamic and kinetic equilibrium at the cooler exit. A cooler efficiency based on a hypothetical optimum cooler was defined. The physical characteristics of an operational exhaust gas spray cooler and the instrumentation systems are described. Experimental measurements obtained from actual cooler operation are compared with the mathematical model predictions. The mathematical model was used over a full range of inlet conditions to calculate cooler exit conditions, and the results are presented. A bibliography of related reports is also presented.

SECTION II
EXHAUST GAS COOLER SYSTEM

2.1 CONFIGURATION

The configuration for a typical horizontal exhaust gas spray cooler consists of a diverging conical inlet section followed by a constant-area duct to the end of the spray cooler (Fig. 1, Appendix I). The cooling water is introduced through groups of nozzles arranged in a series of banks (Fig. 2a), in which the first several banks of sprays consist of nozzles projecting a fan-type spray directed downstream along the wall to protect the ducting (Fig. 2b). The other banks consist of spray heads arranged in a wagon-wheel configuration with several spokes, each "spoke" containing several spray heads. Each spray head contains several fixed-geometry, conical spray nozzles (Fig. 2c) directed generally downstream. The water is supplied by a large header, and each spray bank is supplied from the header by a line containing a valve for flow control.

2.2 INSTRUMENTATION

Instrumentation was provided to measure flow rates, pressures, and temperatures of the exhaust gas stream entering and leaving the cooler; the cooling water into the spray cooler; and the drain water out of the cooler at the cooler drain line. The location of this instrumentation is shown in Fig. 3. Measurements taken by this instrumentation provided information which was used to provide experimental correlation with the analytical results from the mathematical model.

The millivolt outputs from the thermocouples and strain-gage-type pressure transducers were recorded on either magnetic tape or by a photographically recording galvanometer-type oscillograph. The magnetic tape data were reduced on a digital computer, and the oscillograph data were reduced manually using electrical calibrations taken prior to testing.

The cooling water flow rates were calculated using the spray nozzle manufacturer's value of discharge coefficient and a measured pressure drop between the supply header around the cooler and an average cooler pressure. This method assumes that the discharge coefficient and the area of the nozzles have not changed appreciably from the original values. The measured pressures were recorded by an oscillograph.

The cooling water leaving the exhaust gas cooler at the exit through the large (14-in.-diam) drain line was measured using a small flowmeter (3/4-in. turbine-type) mounted as a probe in the drain line. The data were recorded by (1) an oscillograph as an analog signal and (2) a frequency signal. The performance of this device was not satisfactory because of the very low flow rates during cooler operation.

SECTION III
DEVELOPMENT OF THE ANALYTICAL MODEL OF THE SPRAY COOLER

The model to predict cooler exit conditions assumes that the exhaust gas, water vapor, and liquid water are in thermodynamic equilibrium and have the same velocity (kinetic equilibrium) at the exit. The derivation of the equations necessary to compute the exit conditions and efficiency of the exhaust gas cooler is outlined below.

3.1 DERIVATION OF EQUATIONS GOVERNING COOLER BEHAVIOR

From given cooler inlet conditions (pressure, temperature, gas velocity and composition and cooling water temperature and velocity), the amount of cooling water necessary to reach a preselected exit temperature is computed in two distinct processes: (1) saturation (evaporation) and (2) dehumidification (recondensation) with the gas remaining saturated. The exit pressure, velocity, and volume flow rate of noncondensable gas is then calculated. The division of the cooler into distinct processes is an idealization of the real process and is done for analytical reasons only. A schematic of the cooler is shown in Fig. 4.

The analysis of the cooler is based on the following assumptions:

1. Thermodynamic and kinetic equilibrium exist between exhaust gas, water vapor, and liquid water at the cooler exit.
2. Exhaust gas and water vapor behave as perfect gases.
3. All cooling water is injected in the axial direction and remains in the stream as vapor or liquid.
4. The flow is one dimensional, and the cooler has a constant cross-sectional area.
5. Drag forces on duct walls and spray water piping are negligible.
6. All cooling water is injected at the same temperature, $T_{w_1} = T_{w_2}$.

The necessary equations are those of conservation of mass, species, momentum, and energy and the equation of state. Figure 5 is a schematic drawing showing the process.

For the saturation (evaporation) process:

Conservation of mass:

$$\dot{m}_{nc_1} + \dot{m}_{w_1} + \dot{m}_{v_1} = \dot{m}_{nc_2} + \dot{m}_{v_2} \tag{1}$$

also

$$\dot{m}_{nc_1} = \dot{m}_{nc_2} = \dot{m}_{nc} = \rho_{nc}\ AV_{nc} \tag{2}$$

and

$$\dot{m}_{w_1} \div \dot{m}_{v_1} = \dot{m}_{v_2} \tag{3}$$

Conservation of momentum:

$$P_1A + (\dot{m}_{v_1} + \dot{m}_{nc_1})V_{nc_1} + \dot{m}_{w_1}\ V_{w_1} = P_2A + (\dot{m}_{v_2} + \dot{m}_{nc_2})V_{nc_2} \tag{4}$$

Conservation of energy:

$$\dot{m}_{v_1}\left(h_{v_1} + \frac{V_{nc_1}^{\ 2}}{2}\right) + \dot{m}_{nc}\left(h_{nc_1} + \frac{V_{nc_1}^{\ 2}}{2}\right) + \dot{m}_{w_1}\left(h_{w_1} + \frac{V_{w_1}^{\ 2}}{2}\right) = \dot{m}_{v_2}\left(h_{v_2} + \frac{V_{nc_2}^{\ 2}}{2}\right) + \dot{m}_{nc_2}\left(h_{nc_2} + \frac{V_{nc_2}^{\ 2}}{2}\right) \tag{5}$$

where assumption (1) has been used.

Equation of state:

$$P = \frac{\rho \bar{R} T}{\bar{m}} \tag{6}$$

For the saturation process, energy Eq. (5) can be written as:

$$\frac{\dot{m}_{v_2}}{\dot{m}_{nc}} = \frac{(h_{nc_1} - h_{nc_2}) + \dfrac{V_{nc_1}^2 - V_{nc_2}^2}{2} + \dfrac{\dot{m}_{v_1}}{\dot{m}_{nc}}\left(h_{v_1} - h_{w_1} + \dfrac{V_{nc_1}^2 - V_{w_1}^2}{2}\right)}{(h_{v_2} - h_{w_1}) + \dfrac{V_{nc_2}^2 - V_{w_1}^2}{2}} \tag{7}$$

where Eq. (3) has been used to eliminate $\dot{m}_{w_1}$.

For the dehumidification process:

Conservation of mass:

$$\dot{m}_{nc_2} + \dot{m}_{w_2} + \dot{m}_{v_2} = \dot{m}_{nc_3} + \dot{m}_{w_3} + \dot{m}_{v_3}$$

also

$$\dot{m}_{nc_2} = \dot{m}_{nc_3} = \dot{m}_{nc} = \rho_{nc} AV_{nc}$$

and

$$\dot{m}_{w_2} + \dot{m}_{v_2} = \dot{m}_{w_3} + \dot{m}_{v_3}$$

Conservation of momentum:

$$P_2A + (\dot{m}_{v_2} + \dot{m}_{nc_2}) V_{nc_2} + \dot{m}_{w_2} V_{w_2} = P_3A + (\dot{m}_{v_3} + \dot{m}_{nc_3} + \dot{m}_{w_3}) V_{nc_3}$$

Conservation of energy:

$$\dot{m}_{v_2}\left(h_{v_2} + \frac{V_{nc_2}^2}{2}\right) + \dot{m}_{nc}\left(h_{nc_2} + \frac{V_{nc_2}^2}{2}\right) + \dot{m}_{w_2}\left(h_{w_2} + \frac{V_{w_2}^2}{2}\right)$$

$$= \dot{m}_{v_3}\left(h_{v_3} + \frac{V_{nc_3}^2}{2}\right) + \dot{m}_{nc}\left(h_{nc_3} + \frac{V_{nc_3}^2}{2}\right) + \dot{m}_{w_3}\left(h_{w_3} + \frac{V_{nc_3}^2}{2}\right)$$

Equation (6) can be written in the form:

$$\frac{\rho_{nc_2}}{\rho_{nc_3}} = \frac{P_{nc_2}}{P_{nc_3}} \frac{T_3}{T_2} \tag{8}$$

Combining Eqs. (2) and (8), squaring, and solving for $V_{nc_3}^2$ give

$$V_{nc_3}^2 = \frac{\rho_{nc_2}^2}{\rho_{nc_3}^2} V_{nc_2}^2 = \left(\frac{P_{nc_2}}{P_{nc_3}} \frac{T_3}{T_2}\right)^2 V_{nc_2}^2 \tag{9}$$

By noting that $\dot{m} = \rho VA$ and using assumptions (1) and (4), the following can be written:

$$\frac{\dot{m}_{v3}}{\dot{m}_{nc}} = \frac{\rho_{v3}}{\rho_{nc3}} = \frac{P_{v_3}\,\bar{m}_v}{P_{nc_3}\,\bar{m}_{nc}} \tag{10}$$

By solving Eq. (3) for $\dot{m}_{w3}$ and substituting Eqs. (9) and (10) along with $\dot{m}_{w3}$ into Eq. (5), the ratio $\dot{m}_{w2}/\dot{m}_{nc}$ can be expressed as:

$$\frac{\dot{m}_{w2}}{\dot{m}_{nc}} = \frac{(h_{nc_2} - h_{nc_3}) - \left[\left(1 + \dfrac{\dot{m}_{v2}}{\dot{m}_{nc}}\right)\left(\dfrac{P_{nc_2}T_3}{P_{nc_3}T_2}\right)^2 - 1\right]\dfrac{V_{nc_2}^{\,2}}{2} - \dfrac{\dot{m}_{v2}}{\dot{m}_{nc}}(h_{w_3} - h_{v_2}) - \dfrac{P_{v_3}\bar{m}_v}{P_{nc_3}\bar{m}_{nc}}(h_{v_3} - h_{w_3})}{(h_{w_3} - h_{w_2}) + \left[\left(\dfrac{P_{nc_2}T_3}{P_{nc_3}T_2}\right)^2 - \left(\dfrac{V_{w_2}}{V_{nc_2}}\right)^2\right]\dfrac{V_{nc_2}^{\,2}}{2}} \tag{11}$$

This is the form of the energy equation to be used for the dehumidification process.

To develop a usable form of the momentum equation, using Eqs. (2), (3), and (4) and dividing by $\dot{m}_{nc}$ produces the expression:

$$P_3 = P_2 + 2q\left[\left(1 + \frac{\dot{m}_{v2}}{\dot{m}_{nc}}\right)\left(1 - \frac{\rho_{nc2}}{\rho_{nc3}}\right) + \frac{\dot{m}_{w2}}{\dot{m}_{nc}}\left(\frac{V_{w2}}{V_{nc2}} + \frac{\rho_{nc2}}{\rho_{nc3}}\right)\right] \tag{12}$$

where

$$q = \frac{\rho_{nc_2} V_{nc_2}^{\,2}}{2}$$

Substitution of Eq. (8) into this equation gives

$$P_3 = P_2 + 2q\left[\left(1 + \frac{\dot{m}_{v2}}{\dot{m}_{nc}}\right)\left(1 - \frac{P_{nc_2}T_3}{P_{nc_3}T_2}\right) + \frac{\dot{m}_{w2}}{\dot{m}_{nc}}\left(\frac{V_{w2}}{V_{nc2}} - \frac{P_{nc_2}T_3}{P_{nc_3}T_2}\right)\right] \tag{13}$$

The partial pressure of the noncondensable gases at the cooler exit is eliminated by applying Dalton's law of partial pressures:

$$P_3 = P_{v_3} + P_{nc_3} \tag{14}$$

At this point the momentum equation is rearranged and placed into quadratic form:

$$aP_3^{\,2} - bP_3 + c = 0 \tag{15}$$

where

$$a = 1$$

$$b = -\left[P_2 + P_{v_3} + 2q\left(1 + \frac{\dot{m}_{w2}}{\dot{m}_{nc}} + \frac{\dot{m}_{w2}}{\dot{m}_{nc}}\,\frac{V_{w2}}{V_{nc2}}\right)\right] \tag{16}$$

and

$$c = 2q\left[1 + \frac{\dot{m}_{w_2}}{\dot{m}_{nc}} + \frac{\dot{m}_{w_2}}{\dot{m}_{nc}} \frac{V_{w_2}}{V_{nc_2}}\right] P_{v_3} - 2q \frac{P_{nc_2} T_3}{T_2} \left(\frac{\dot{m}_{w_2}}{\dot{m}_{nc}} + 1 + \frac{\dot{m}_{w_2}}{\dot{m}_{nc}}\right) + P_2 P_{v_3} \quad (16)$$

The roots of the quadratic have the form

$$P_3 = \frac{-b \pm \sqrt{b^2 - 4ac}}{2a} \quad (17)$$

where only the (+) sign has physical meaning. In summary, the equations to be solved are Eqs. (7) or (11) and (17) and the following conditions are known:

1. The enthalpy of all constituents as a function of temperature only.
2. The partial pressure of water as a function of temperature.
3. The temperature, pressure, and velocity of the exhaust gas entering the cooler, and the temperature and velocity of the cooling water being sprayed into the gas stream.

The procedure used by the computer to solve the equations is given in Appendix III.

3.2 "OPTIMUM" COOLER

An "ideal" cooler may be defined by the same assumptions as used for the equilibrium model except that:

1. The static pressure will be constant in the cooler, and
2. All liquid water (recondensed and sprayed) will be removed from the stream when it has achieved thermodynamic equilibrium.

A theoretical cooler efficiency may then be defined as the ratio of the cooling water required for this ideal cooler to that determined by the equilibrium calculations at conditions of equal volume flow rates at the cooler exit.

$$\eta_{theo} = \frac{\dot{m}_{w\ ideal}}{\dot{m}_{w\ equilibrium}} \quad (18)$$

The requirement of equal volumetric flow rates was made because this condition is believed to agree with conditions in ETF.

The equilibrium analysis has been presented in the previous section. The idealized equations are developed in this section and, because of their ultimate use in determining cooler theoretical efficiency, just described, are called "efficiency equations."

The idealization assumes that:

1. The cooler operates with a constant static pressure ($P_1 = P_2 = P$), and
2. All previous assumptions are valid except that, after saturation is initially achieved, all liquid water is removed from the stream after coming to thermodynamic equilibrium.

Writing mass and heat balance equations for the cooler gives:

Mass balance:

$$\dot{m}_{nc_1} + \dot{m}_{v_1} + \dot{m}_{w_1} = \dot{m}_{nc_2} + \dot{m}_{v_2} \tag{19}$$

but

$$\dot{m}_{nc_1} = \dot{m}_{nc_2} \tag{20}$$

therefore,

$$\dot{m}_{v_1} + \dot{m}_{w_1} = \dot{m}_{v_2} \tag{21}$$

Energy balance:

$$\dot{m}_{nc}\, h_{nc_1} + \dot{m}_{v_1} h_{v_1} + \dot{m}_{w_1} h_{w_1} = \dot{m}_{nc}\, h_{nc_2} + \dot{m}_{v_2} h_{v_2} \tag{22}$$

Equations (21) and (22) can be combined to yield

$$h_{nc_2} - h_{nc_1} = \dot{m}_{v_2}/\dot{m}_{nc}\,(h_{v_1} - h_{v_2}) + \dot{m}_{w_1}/\dot{m}_{nc}\,(h_{w_1} - h_{v_1}) \tag{23}$$

Substituting Dalton's Law [Eq. (14)] into Eq. (10) gives

$$\frac{\dot{m}_{v_2}}{\dot{m}_{nc}} = \frac{\rho_{v_2}}{\rho_{nc_2}} = \frac{P_{v_2}}{(P - P_{v_2})}\ \frac{\overline{m}_v}{\overline{m}_{nc}} \tag{24}$$

Using the continuity equation (21) and solving for the ratio P_{v_2}/P give

$$\frac{P_{v_2}}{P} = \frac{\overline{m}_{nc}\left(\dfrac{\dot{m}_{w_1}}{\dot{m}_{nc}} + \dfrac{\dot{m}_{v_1}}{\dot{m}_{nc}}\right)}{\overline{m}_v + \left(\dfrac{\dot{m}_{w_1}}{\dot{m}_{nc}} + \dfrac{\dot{m}_{v_1}}{\dot{m}_{nc}}\right)\overline{m}_{nc}} \tag{25}$$

Substituting Eq. (24) into Eq. (23) gives

$$h_{nc_2} - h_{nc_1} = \frac{P_{v_2}\,\bar{m}_v}{(P - P_{v_2})\,\bar{m}_{nc}}\,(h_{v_1} - h_{v_2}) + \frac{\dot{m}_{w_1}}{\dot{m}_{nc}}\,(h_{w_1} - h_{v_1}) \tag{26}$$

Equation (25) can be solved for $\dfrac{\dot{m}_{w_1}}{\dot{m}_{nc}}$:

$$\frac{\dot{m}_{w_1}}{\dot{m}_{nc}} = \frac{\left(1 - \dfrac{P_{v_2}}{P}\right)\left(\dfrac{\bar{m}_v}{\bar{m}_{nc}} + \dfrac{\dot{m}_{v_1}}{\dot{m}_{nc}}\right) - \dfrac{\bar{m}_v}{\bar{m}_{nc}}}{\dfrac{P_{v_2}}{P} - 1} \tag{27}$$

This ratio is used in Eq. (26), and P_{v_2} is solved for:

$$P_{v_2} = P\left[\frac{h_{nc_2} - h_{nc_1} + \dfrac{\dot{m}_{v_1}}{\dot{m}_{nc}}\,(h_{w_1} - h_{v_1})}{h_{nc_2} - h_{nc_1} + \dfrac{\bar{m}_v}{\bar{m}_{nc}}\,(h_{v_1} - h_{v_2}) + \left(\dfrac{\bar{m}_v}{\bar{m}_{nc}} + \dfrac{\dot{m}_{v_1}}{\dot{m}_{nc}}\right)(h_{w_1} - h_{v_1})}\right] \tag{28}$$

The dehumidification section for the ideal cooler is represented by a series of differential elements in which water is allowed to reach thermodynamic equilibrium with the gas phase and the recondensed water is removed before advancing to the next differential element. Each differential element corresponds to a dT. A schematic diagram is shown in Fig. 6 for a single typical element.

For a differential element, the equations for the conservation of mass and energy can be written:

Mass:

$$d\dot{m}_{w_2} = d\dot{m}_v + d\dot{m}_{w_D} \tag{29}$$

Energy:

$$\dot{m}_{nc}\,dh_{nc} = h_{w_2}\,d\dot{m}_{w_2} - \dot{m}_v\,dh_v - h_v\,d\dot{m}_v - h_{w_D}\,d\dot{m}_{w_D} \tag{30}$$

Substituting for $d\dot{m}_{w_D}$ from Eq. (29) into Eq. (30) and solving for dh_{nc} give

$$dh_{nc} = (h_{w_1} - h_{w_D})\,\frac{d\dot{m}_{w_1}}{\dot{m}_{nc}} - \frac{\dot{m}_v}{\dot{m}_{nc}}\,dh_v - (h_v - h_{w_D})\,\frac{d\dot{m}_v}{\dot{m}_{nc}} \tag{31}$$

If $P_v = P_{v_s} = f(T)$ throughout the dehumidification section, Eq. (24) may be written as

$$\frac{\dot{m}_v}{\dot{m}_{nc}} = \frac{P_{v_s}}{(P - P_{v_s})} \frac{\bar{m}_v}{\bar{m}_{nc}} \tag{32}$$

or

$$\frac{d\dot{m}_v}{\dot{m}_{nc}} = \frac{\bar{m}_v}{\bar{m}_{nc}} \, d\left(\frac{\bar{m}_v}{P - P_{v_s}}\right) \tag{33}$$

By substituting Eqs. (32) and (33) into Eq. (31) and defining

$$dF = \frac{d\dot{m}_{w1}}{\dot{m}_{nc}} \tag{34}$$

Eq. (31) becomes

$$dF = \frac{dh_{nc}}{h_{w_1} - h_{w_D}} + \frac{P_{v_s}}{P - P_{v_s}} \frac{\bar{m}_v}{\bar{m}_{nc}} \frac{dh_v}{h_{w1} - h_{w_D}} + \left(\frac{h_v - h_{w_D}}{h_{w1} - h_{w_D}}\right)\left(\frac{\bar{m}_v}{\bar{m}_{nc}}\right) d\left(\frac{P_{v_s}}{P - P_{v_s}}\right) \tag{35}$$

Equation (35) may be simplified by introducing

$$h_{w_2} - h_{w_D} = T_{w_2} - T \qquad \text{Note: } c_{p_w} = 1 \tag{36}$$

and

$$h_v - h_{w_D} = h_{fg} \tag{37}$$

Equation (35) in integrated form is

$$F = \int_{T_2}^{T} \left[\frac{1}{T_{w_2} - T} \frac{dh_{nc}}{dT} + \frac{P_{v_s}}{P - P_{v_s}} \frac{\bar{m}_v}{(\bar{m}_{nc})(T_{w_2} - T)} \frac{dh_v}{dT} + \frac{h_{fg}}{T_{w_2} - T} \frac{\bar{m}_v}{\bar{m}_{nc}} \frac{d}{dT}\left(\frac{P_{v_s}}{P - P_{v_s}}\right)\right] dT \tag{38}$$

Equation (38) may be solved by using h_{nc}, P_{v_s}, h_v, and h_{fg} each as a function of T.

SECTION IV
ANALYTICAL MODEL APPLICATION

The equilibrium and efficiency equations for the spray cooler were programmed in FORTRAN IV language for computer solution. Combustion equilibrium calculations were separately performed to establish

the cooler inlet states using the method of Ref. 3. These included the molecular weights, species mass fractions, volume of the noncondensable gas, and the gas temperatures based on certain fuel/air ratios of conventional hydrocarbon turbojet fuels.

An exploratory series of computer runs was made to observe the effect of varying one parameter at a time in the equations. In this way, results can be observed in a qualitative manner. A realistic grid was selected covering a range of experimental data for both the independent and fixed inlet conditions. The range of the assigned values is indicated as Cases I through V in Table I (Appendix II)

4.1 PROGRAM OUTPUT AND TYPICAL RESULTS

The computer program generated printouts of selected parameters and graphs. These parameters included T_3, P_3, P_{v3}/P_3, V_{nc3}, $\dot{m}_{v1}/\dot{m}_{nc}$, and $Q/\dot{m}_{nc}$.

Preliminary computer runs indicated some difficulties with allowing the calculations to proceed to the temperature $T_3 = T_{w1}$. Solution of Eq. (17) presents the possibility of a negative discriminant. Additional discussion of this negative discriminant and the required constraint on the program is presented in Appendix IV.

The results of the computer calculations are shown in Figs. 7 through 11.

As the temperature of the cooling water is decreased, the temperature of the exhaust gas at the exit of the cooler also decreases for a fixed amount of water injected (see Fig. 7). In addition, the pressure drop across the cooler decreases as the cooling water temperature decreases. Therefore, within the constraints of the model, where high temperature exhaust gas may be generated and the pressure drop across the cooler may be critical, testing should be conducted using the lowest temperature cooling water possible.

The second variable investigated was the influence of the cooling water injection velocity on the exit temperature and pressure (Fig. 8). The injected water velocity has negligible effect on the final gas temperature for a fixed amount of cooling water injected since the kinetic energy of this item is almost negligible itself especially at the lower values of m_{w1}/m_{nc}. Increasing the injection velocity will decrease the pressure drop. This would be expected since the cooling water

possesses more momentum and requires less contribution from the gas stream for its acceleration to equilibrium conditions.

The effect of decreasing the cooler inlet pressure while the remaining inlet conditions remain fixed is shown in Fig. 9. The pronounced effect on the exit temperature at initial saturation conditions is caused by the low saturation temperature at the lower values of partial pressure. For the initial conditions used, the cooling process is essentially constant pressure, and lowering the inlet pressure does not appreciably change this.

The effect of increasing the inlet gas velocity is shown in Fig. 10. The general shape of the exit temperature and pressure curve is similar to that of Fig. 8 where the velocity of the injected cooling water is varied. In both cases, the exit temperature and pressure decrease as the velocity difference between exhaust gas and inlet cooling water increase. It can also be seen in Fig. 10 that as the velocity increases there is a maximum amount of cooling water ($m_{w_{1,2}}/m_{nc}$) that can be injected and still have equilibrium conditions at the exit. This also places a minimum value on the exit temperature of the exhaust gas. The physical significance of this limit is discussed in Appendix III.

The final variable used in the study was inlet exhaust gas temperature. This was varied from 1048 to 4057°R, and the exit temperature and pressure were determined at various values of cooling water flow rate ($m_{w_{1,2}}/m_{nc}$). For a predetermined value of $m_{w_{1,2}}/m_{nc}$, the lower the inlet temperature, the lower the exit temperature (Fig. 11). The exit pressure decreased as the inlet temperature decreased, also for a predetermined value of $\dot{m}_{w_{1,2}}/m_{nc}$. The decrease in pressure at a lower inlet temperature was because a smaller quantity of water was vaporized and therefore a negligible increase in stagnation pressure resulted (A discussion of the effects of mass additions on stagnation pressure may be found in Chapter 8 of Ref. 4). Also there was more liquid water remaining in the stream to accelerate to kinetic equilibrium at the lower values of temperature.

4.2 KINETIC EQUILIBRIUM

An assumption made when deriving the equations for the spray cooler performance program was that the flow is in kinetic and thermodynamic equilibrium at the cooler exit. To determine the effect of assuming kinetic equilibrium, a typical set of cooler conditions was

chosen, and the usual parameters T_3, P_3, and $\dot{m}_{w1+2}/\dot{m}_{nc}$ were obtained, as well as the six individual terms of the momentum equation in the following form:

$$\frac{P_1 A_1}{\dot{m}_{nc}} + \left(\frac{\dot{m}_{v1}}{\dot{m}_{nc}} + 1\right)\frac{V_{nc_1}}{g_c} + \frac{\dot{m}_{w1}}{\dot{m}_{nc}}\frac{V_{w1}}{g_c} = \frac{P_3 A_3}{\dot{m}_{nc}} + \left(\frac{\dot{m}_{v3}}{\dot{m}_{nc}} + 1\right)\frac{V_{nc3}}{g_c} + \frac{\dot{m}_{w3}}{\dot{m}_{nc}}\frac{V_{nc3}}{g_c}$$

where

$$\frac{P_1 A_1}{\dot{m}_{nc}} = \frac{P_1 A_1}{\rho_{nc_1} V_{nc_1} A_1} = \frac{P_1}{\rho_{nc_1} V_{nc_1}} = \frac{P_1 R_{nc} T_1}{P_{nc_1} V_{nc_1}}$$

and similarly

$$\frac{P_3 A_3}{\dot{m}_{nc}} = \frac{P_3 R_{nc} T_3}{P_{nc_3} V_{nc_3}}$$

The assumption of kinetic equilibrium requires that the liquid water must be accelerated to the gas velocity leaving the cooler. Therefore, the relative weight of the water term $(\dot{m}_{w3}/\dot{m}_{nc})(V_{nc_3}/g)$ was observed. The inlet parameters were:

$$P_1 = 6 \text{ psia}$$

$$T_1 = 2718^\circ R$$

$$T_{w_1} = 520^\circ R$$

$$V_{w_1} = 100 \text{ ft/sec}$$

$$V_{g_1} = 480 \text{ ft/sec}$$

and

$$\dot{m}_{nc} = 1 \text{ lbm/sec}$$

Table II contains values of the individual terms which comprise the momentum equation and their respective values as $\dot{m}_{w1,\,2}/\dot{m}_{nc}$ varied. The right hand column gives the contribution of the term $(\dot{m}_{w3}/\dot{m}_{nc})(V_{nc3}/g)$ to the total momentum as the cooling water ratio $(\dot{m}_{w1,\,2}/\dot{m}_{nc})$ varied. Since assuming kinetic equilibrium (i. e., $V_{w3} = V_{nc3}$) is the limiting case, the percentages shown are the maximum contributions of the liquid water at the exit when assumed to be in kinetic equilibrium. If the value of the water term were less, the effect would be smaller.

Experience to date has shown that a value of approximately five or less for the ratio $\dot{m}_{w1+2}/\dot{m}_{nc}$ is sufficient for the majority of turbojet

testing conditions. Thus, for the case presented in Table II, the term directly associated with kinetic equilibrium is seen to carry approximately 6 percent of the total momentum. It is concluded that the assumption of kinetic equilibrium at the spray cooler exit is a justifiable one for many cases and that the prediction of the exit pressure would be incorrect by no more than 6 percent. This amount of error would probably be higher for low pressure or high subsonic conditions.

4.3 THERMODYNAMIC EQUILIBRIUM

A study was also made to check the effect of assuming thermodynamic equilibrium. Assuming equilibrium in this manner means that the temperatures of all constituents (noncondensable exhaust gas, water vapor, and liquid water) are equal as well as the partial pressures of liquid water and vapor as they pass the exit plane of the cooler. Since the final temperature of the liquid water (T_{w_3}) is a function of many items outside the scope of this computer program (such as nonequilibrium effects), this parameter was arbitrarily varied to determine the effect on the required water for cooling ($\dot{m}_{w_{1,2}}/\dot{m}_{nc}$). The temperature of the water at station 3 (T_{w_3}) was taken to be:

$$T_{w_3} = T_{nc_3} - (T_{nc_3} - T_{w_1})\,X$$

where X was equal to 0, 0.1, 0.5, and 0.7. The limiting case is X = 0, which is the assumption of thermodynamic equilibrium. The partial pressure of the water vapor was taken to be a function of T_{nc_3}. The amount of water required to cool the engine exhaust gas is extremely sensitive to the final water temperature (T_{w_3}) as shown in Fig. 12. The input conditions were the same as for the previous kinetic equilibrium case. To cool the exhaust gas to 590°R would require the mass ratio of water to noncondensable gas to vary from approximately 4 to 12 for X varying from 0 to 0.7, respectively. Hence, the cooler performance is very sensitive to the degree of thermodynamic nonequilibrium at the exit. An accurate independent measurement of the water and exhaust gas temperatures is essential for determining the true state of the exhaust gas at the exit.

4.4 EFFICIENCY OF AN EXPERIMENTAL COOLER

To show the effects on the theoretical efficiency, $\eta_{theo} = \dfrac{\dot{m}_{w\ optimum}}{\dot{m}_{w\ equilibrium}}$, of varying the parameters T_{w_1} and V_{w_1}, the limiting values were selected from Case I and the limiting and mean

values from Case II, respectively. In Fig. 13a, T_{w1} has the values of 500 and 545°R which experience has shown are the lower and upper limits of the cooling water inlet temperature in the AEDC coolers of interest. As would be expected, the lower water temperature yields a higher efficiency for a given volume flow rate. Figure 13b shows how V_{w1} can affect the efficiency; V_{w1} took the values 50, 90, and 130 ft/sec. For a given volume flow rate, the efficiency is greatest at the highest water velocity. This is to be expected. High water velocity means less momentum lost by the exhaust gas and, therefore, a situation closer to the "ideal" as defined by constant pressure throughout the cooler.

The theoretical efficiency (η_{theo}) establishes a ratio of optimum to equilibrium conditions. The actual efficiency (η_{actual}) establishes a ratio of ideal to actual conditions. The efficiency ratio ($\eta_{actual}/\eta_{theo}$) establishes a ratio of actual to theoretical efficiencies resulting in a measure of attainment of the actual case to the equilibrium case. This provides comparison of actual test conditions with the ideal equilibrium conditions and, as such, is a measure of effectiveness of actual operation.

To develop this efficiency ratio ($\eta_{actual}/\eta_{theo}$), three experimental tests were selected on the basis of having approximately constant cooler inlet conditions (see Table III) and assumed equilibrium outlet conditions. With the latter assumption and measuring the necessary inlet conditions (noncondensable and cooling water flow rates) and exit conditions (pressure and temperature), the volumetric flow rate of the exhaust gas at the exit is calculated. The temperature is measured with a bare wire thermocouple extending into the gas stream where it will record the temperature of the liquid water impinging on it. Since equilibrium has been assumed, this will also be the gas temperature. The amount of cooling water necessary to give this volumetric flow rate is calculated using the equilibrium and "optimum" cooler computer programs. The theoretical efficiency ($\eta_{theo} = \dot{m}_{w_{optimum}}/\dot{m}_{w_{equilibrium}}$) as a function of the cooling water ratio ($\dot{m}_{w1+2}/\dot{m}_{nc}$) is shown for each experimental measurement separately (Fig. 13c). This shows the maximum achievable efficiency based on the equilibrium assumptions and the actual efficiency based on measured values. The ratio of actual to theoretical efficiencies is shown in Fig. 13d to indicate how close to equilibrium efficiency the existing coolers are operating. It can be seen that the cooler operates close to maximum predicted efficiency at the lower values of $\dot{m}_{w1+2}/\dot{m}_{nc}$ but decreases as the value of $\dot{m}_{w1+2}/\dot{m}_{nc}$ increases.

SECTION V
CONCLUDING REMARKS

Testing of turbojet engines and rocket motors at the ETF requires the cooling of hot exhaust gases, and direct contact water sprays are used for cooling. To facilitate the understanding of the cooling process, an analytical model of an exhaust gas spray cooler was developed. Results from the model were used to compare with measurements made during actual engine tests. The analytical model as developed includes the equilibrium equations and "ideal" efficiency equations and is based on the assumptions of: (1) thermodynamic and kinetic equilibrium at the exit, (2) perfect gases and vapor, (3) all cooling water remaining in the stream flow, (4) one-dimensional constant area flow, (5) no external drag forces, and (6) discrete saturation and dehumidification processes. The method of solution of these equations has been outlined in the form in which they were programmed for the computer.

The computer program gives an opportunity to evaluate the influence of various parameters on the output. The analytical examination of the kinetic and thermal equilibrium assumptions show that the calculation of cooler exit conditions is relatively insensitive to kinetic equilibrium, but sensitive to the degree of thermal nonequilibrium. Efficiency calculations confirm that two contributing items to higher efficiency are low water temperature and high water velocity. Experimental measurements indicate that the efficiency is closer to theoretical at low values of $\dot{m}_{w1+2}/\dot{m}_{nc}$ than at the higher values.

Verification of the validity of the analytical model assumptions regarding exit equilibrium conditions will require development of new instrumentation for two-phase flow conditions. Further refinement of the analytical model will be required to incorporate consideration of droplet size and distribution, and nonequilibrium thermodynamic effects.

REFERENCES

1. Nitsch, J. "First Considerations on the Calculation of Heat and Material Exchange in Injector Coolers with Aid of Model Representation." DVL Internal Report No. 92.

2. Nitsch, J. "A Model of the Calculation of the Thermodynamic Process of Exhaust Gas Cooling with Injection Coolers." DVL Internal Report No. 101, April 1968.

3. McBride, Bonnie J. and Gordon, Sanford. "Fortran IV Program for Calculation of Thermodynamic Data." NASA TN D-4097, August 1967.

4. Shapiro, A. H. The Dynamics and Thermodynamics of Compressible Fluid Flow. Vol. I, Ronald Press Company, New York, 1953.

BIBLIOGRAPHY

1. Ackermann, G. "Heat Transfer and Molecular Transfer in the Same Field with High Temperature and Partial Pressure Differences." VDI-Forschungsheft 382, Berlin 1937.

2. Adelberg, M. "Breakup Rate and Penetration of a Liquid Jet in a Gas Stream." AIAA Journal, Vol. 5, No. 8, pp. 1408-1415, August 1967.

3. "An Investigation of Evaporative Cooling of a High Velocity Air Stream in a 5-Inch Diameter Duct Using Single Water-Injection Nozzles." G. L. Martin Company, ER 7937 (AD301329), March 1956.

4. Andeen, G. B. and Griffith, P. "Momentum Flux in Two-Phase Flow." Journal of Heat Transfer, p. 211, May 1968.

5. Bosnjakovic, F. Technical Thermodynamics. Translated by P. L. Blackshear. Holt, Rinehart, and Winston, New York, 1965.

6. Bitron, M. D. "Atomization of Liquids by Supersonic Air Jets." Ind. and Eng. Chem., Vol. 47, No. 1, p 23, January 1955.

7. Bittker, D. A. "Effect of Ambient Air Velocity on Atomization of Two Impinging Water Jets." NASA TND-2087, February 1964.

8. Chilton, T. H. and Colburn, A. P. "Distillation and Adsorption in Packed Columns." Industrial and Engineering Chemistry, Vol. 27, No. 3, pp. 255-260, March 1935.

9. Chilton, T. H. and Colburn, A. P. "Mass Transfer (Adsorption) Coefficients." Ind. and Eng. Chem., Vol. 26, No. 11, pp. 1183-1187, November 1934.

10. Colburn, A. P. and Drew, T. B. "Condensation of Mixed Vapors." Transaction of AICHE, Vol. 33, p. 167, 1937.

11. Crowe, C. T., Nicholls, J. A., and Morrison, R. B. "Drag Coefficient of Inert and Burning Particles Accelerating in Gas Streams." Presented at Ninth International Symposium on Combustion, Cornell University, August 27 to September 1, 1962.

12. DeJuhasz, K. J. Spray Literature Abstracts. Vol. I, 1959, Vol. II, 1964, ASME Publication.

13. DeLeo, R. V. "Dehumidification of Air Vapor Mixtures of High Specific Humidity by Water Injection." University of Minnesota, Rosemont Aeronautical Laboratory RR-82, July 1952.

14. Janus Products, Inc. "Design Study and Functional Requirements for Tripltee." AEDC-TR-65-180 (AD469042L), August 1965.

15. Dickerson, R., Tate, K., and Barsic, N. "Correlation of Spray Injector Parameters with Rocket Engine Performance." AFRPL-TR-68-147 (AD824371), June 1968.

16. Dukler, A. E., Wicks, M., and Cleveland, R. G. "Frictional Pressure Drop in Two-Phase Flow: B. An Approach through Similarity Analysis." AICHE Journal, p. 44, January 1964, and "A. A Comparison of Existing Correlations for Pressure Loss and Holdup." AICHE Journal, p. 38, January 1964.

17. Eckert, E. R. G. and Drake, R. M., Jr. Heat and Mass Transfer. McGraw-Hill, New York, 1959.

18. Eckert, E. R. G. and Drake, R. M., Jr. Introduction to Heat and Mass Transfer. Translated by J. F. Gross. McGraw-Hill, New York, 1963.

19. Eckert, E. R. G. and Drake, R. M., Jr. Introduction to the Transfer of Heat and Mass. McGraw-Hill, New York, 1950.

20. Elliott, D. G. and Weinberg, E. "Acceleration of Liquids in Two-Phase Nozzles." JPL/CIT TR 32-987, July 1968.

21. English, R. E. and Wachtl, W. W. "Charts of Thermodynamic Properties of Air and Combustion Products from 300° to 3500°R, NACA TN 2071, April 1950.

22. Erickson, A. J. "A Theoretical and Experimental Investigation of the Aerothermopressor Process." Gas Turbine Laboratory, M. I. T., (AD200658), May 1958.

23. "Exhaust Gas Spray Cooler Bibliography." Volume 1. ARB-003469, Defense Document Center, November 1968.

24. Felder, H. and Herzke, J. "Interim Report Concerning an Investigation of Exhaust Gas Cooling at about 0.1 atm with Water Streams and Water Droplets." Porz-Wahn, German Research Institution for Air and Space Travel. Institute for Airflow Studies, April 1965. Translated by C. Henn, ARO, Inc., June 1965.

25. Felder, H. and Herzke, J. "Investigation on the Cooling of Exhaust Gas by Direct Contact between Exhaust Gas and Water." DLR-FB-67-15 (AD816794), March 1967.

26. Gavril, Bruce D. "A Theoretical Investigation of the Thermodynamic and Dynamic Effects of Water Injection into High Velocity High Temperature Gas Stream." Thesis for ScD in M. E., Massachusetts Institute of Technology, Cambridge, Massachusetts, June 1954.

27. Godsave, G. A. E. "The Burning of Single Drops of Fuel." Fourth Symposium on Combustion. Published by Wilkins and Wilkins, Baltimore, Maryland, pp. 818-830, 1953.

28. Gordon, J. S. "Thermodynamics of High Temperature Gas Mixtures, and Application to Combustion Problems." WADC TR 57-33 (AD110735), January 1957.

29. Grabau, M. and Brahinsky, H. S. "Thermodynamic Properties of Air from 300 to 6000°K and from 1 to 1000 Amagats." AEDC-TR-66-247 (AD646172), January 1967

30. Grober, H. and Erk, S. Fundamentals of Heat Transfer. Translated by J. R. Moszynski. McGraw-Hill, New York, 1961.

31. Grouse, S. W., Jr. "An Index to the Two-Phase Gas-Liquid Flow Literature." MIT Report No. 9, The MIT Press, 1966.

32. Handbook of Supersonic Aerodynamics. Section 4--The Mechanics and Thermodynamics of Steady One-Dimensional Gas Flow, Bureau Ordnance, Department of the Navy, NAVORD Report 1488, Vol. 1, 1950.

33. Harmon, D. B., Jr. "An Equation for Predicting a Medium Size Drop Size in a High Speed Spray." Univ. Cal. Publications in Engineering, Vol. 5, No. 5, pp. 145-158, 1955.

34. Harrje, D. T., et al. "Nonlinear Aspects of Combustion Instability in Liquid Propellant Rocket Motors." NASA CR 72426, June 1968.

35. Hensley, R. V. "Mollier Diagrams for Air Saturated with Water Vapor at Low Temperatures." NACA TN 1715, September 1948.

36. Heidmann, M. F. and Foster, H. H. "Effect of Impingement Angle on Drop Size Distribution and Spray Pattern of Two Impinging Water Jets." NASA TND-872, July 1961.

37. Hobler, T. Mass Transfer and Absorbers. Translated from Polish by Dr. J. Bandrowski (TP 156M3H6) Pergamon Press, 1966.

38. Hopkins, D. F. "A Study of Fluid Jet Penetration." Ph. D. Dissertation University Illinois, 62-6162 University Microfilm, 1962.

39. Huff, V. N. and Gordon, S. "Tables of Thermodynamic Functions for Analysis of Aircraft-Propulsion Systems." NACA TN 2161, August 1950.

40. Ingebo, R. D. "Vaporization Rates and Heat-Transfer Coefficients for Pure Liquid Drops." NACA TN 2368, July 1951.

41. Ingebo, R. D. "Vaporization Rates and Drag Coefficients for Isooctane Sprays in Turbulent Air Streams." NACA TN 3265, October 1954.

42. Ingebo, R. D. and Foster, H. H. "Drop-Size Distribution for Crosscurrent Breakup of Liquid Jets in Airstreams." NACA TN 4087, October 1957.

43. Jahnke-Emde-Lösch. "Tables of Higher Functions." 6 Aufl., 1960, BG Teubner, Stuttgart.

44. Kays, W. M. Convective Heat and Mass Transfer. McGraw-Hill, New York, 1966.

45. Kolodner, Ignace I. "Growth of Drops by Condensation." IMM-NYU 215 (AD121943), March 1955.

46. Kumm, E. L. "Calculations on the Evaporative Rate of Sprays in Rapidly Moving Gas Streams." AII 60 069. NAA AL-916 June 23, 1949.

47. Levy, J. "The Mixing of Vapor and Liquid Jets." R-1344 (AD152896), October 15, 1957.

48. Lockhart, R. W. and Martinelli, R. C. "Proposed Correlation of Data for Isothermal Two-Phase Two-Compact Flow in Pipes." Chemical Engineering Progress, Vol. 45, No. 1, p. 39, January 1949.

49. Mathews, B. J., Wuerker, R. F., and Harrje, D. T. "Small Droplet Measuring Technique." AFRPL-TR-68-156, July 1968.

50. Mehserle, Henry James. "The Design and Development of a Hele-Shaw Apparatus for Flow Visualization." USAFIT Thesis, GAE/AE/61-6 (AD268696), August 1961.

51. Michejew. Basic Heat Transfer. VEB, Berlin, 1962.

52. Miesse, C. C. "A Theory of Spray Combustion." Ind. and Eng.. Chem., Vol. 50, No. 9, p. 1303, September 1958.

53. Miesse, C. C. "Effect of High Altitude Conditions on Atomization Phenomena." Jet Propulsion, pp. 335-337, May 1958.

54. Miesse, C. C. "One-Dimensional Velocity Variation of a Burning Droplet." Heat-Transfer and Fluid Mechanics Institute, American Society of Mechanical Engineers, May 1953.

55. Miesse, C. C. "Recent Advances in Spray Technology." Applied Mechanics Reviews, Vol. 9, No. 8, p. 321, August 1955.

56. Miesse, C. C. "The Effect of a Variable Evaporation Rate on the Ballistics of Droplets." Franklin Instrument Journal, pp. 391-401, November 1957.

57. Mugele, R. A. and Evans, H. D. "Droplet Size Distribution in Sprays." Ind. and Eng. Chem., pp. 1317 to 1324, June 1951.

58. Norman, W. S. Absorption, Distillation and Cooling Towers. Longmans, 1961.

59. Nukiyama, Shiro and Tanasawa, Yasushi. "Experiments on the Atomization and Liquids in an Air Stream." Reports 1 to 6. Translated from the Transactions of the Society Mechanical Engineers (Japan), Vol. 4, 5, 6, 1938-40 by E. Hope, Canada Department of National Defense, Defense Research Board, Report EO/2820, Ottawa, Canada, March 18, 1950.

60. Penner, S. S. "Chemical Problems in Jet Propulsion." Pergamon Press, New York, 1957.

61. Penner, S. S. and Ta Li. "Thermodynamic Considerations of Droplets and Bubbles." AIAA Journal, Vol. 5, No. 8, pp. 1528 and 1529, August 1967.

62. Petrazhitskiy, G. B. "Experimental Investigation of Droplet Vaporization under Conditions of High Temperatures and Pressures." NASA TT F-266, November 1964.

63. Plank, R. Handbook of Cold Technology. Bd. 3, 1959, Springer-Verlag, Berlin.

64. Ranz, W. E. and Marshall, W. R. "Evaporation from Drops." Chemical Engineering Progress, Vol. 48, pp. 141, 146, 173, 180, Part I--March 1952, Part II--April 1952.

65. Sartell, P. M. "Vapor Capacity Chart." WADC-TN-56-69, Supplement 1 (AD96085), May 1957.

66. Schuyler, F. L. "Combustion Instability; Liquid Stream and Droplet Behavior, Part I, Experimental and Theoretical Analysis of Evaporating Droplets." WADC TR 59-720 (AD247151), September 1960.

67. Shaffer, W. L. "An Analytical Evaluation of the Impingement of Air-Borne Water Particles on a 90-degree Turning Vane." AEDC-TDR-63-195 (AD418994), October 1963.

68. Shapiro, A. H., Wadleigh, K. R., Gavril, B. D., and Fowle, A. A. "The Aerothermopressor--A Device for Improving the Performance of a Gas-Turbine Power Plant." Trans. ASME, April 1956.

69. Skrotzki, Bernhardt G. Basic Thermodynamics. McGraw-Hill, New York, 1963.

70. Smith, F. H., Jr. "Analytical Methods for the Design of Multistage Gas-Driven Ejector Systems with Interstage Cooling." AEDC-TR-65-139 (AD467444), August 1965.

71. Starrett, P. S., and Nottage, H. B., et al. "Survey of Information Concerning the Effects of Non Standard Approach Conditions upon Orifice and Venturi Meters." 65-WA/FM-5, ASME.

72. Table of the Thermal Properties of Gases. Circular 564, National Bureau of Standards, 1955.

73. Tate, R. W. and Marshall, W. R. "Atomization of Centrifugal Pressure Methods." Chemical Engineering Progress, Vol. 49, p. 169, April 1953, Part II, Chemical Engineering Progress, Vol. 49, No. 5, p. 226, May 1953.

74. The Penn State Bibliography on Sprays. Second Edition, The Texas Co., TC 173, p. 4, 1953.

75. Tribus, M., Klein, J. S., and Rembowski, J. "A Method for Calculating the Rate of Evaporation and the Change in Drop Size Distribution for Pure Sprays Injected into Unsaturated Air." University of Michigan, Engineering Research Institute, WADC, ATI 168524, May 1952.

76. Turner, G. M. and Moulton, R. W. "Drop Size Distribution from Spray Nozzles." Chemical Engineering Progress, Vol. 49, No. 4, p. 185, April 1953.

77. Walls, H. A. and Lamb, J. P. "Two-Phase Flow in Spray Coolers." AEDC-TR-68-127 (AD671118), June 1968.

78. "Water Jet Penetration of a High Velocity Gas Stream in Cross Flow." Aerojet General, RN-TM-0559, December 1967.

79. West, R. G. "The Problems of Non Standard Installations and Some General Conclusions." Instrument Practice, p. 973, August 1961.

80. Wilcox, E. C. "Turbojet Thrust Augmentation by Evaporation of Water Prior to Mechanical Compression as Determined by Use of Psychrometric Chart." NACA TN 2105, June 1950.

81. Wilcox, E. C. and Trout, A. M. "Analysis of Thrust Augmentation of Turbojet Engines by Water Injection at Compressor Inlet Including Charts for Calculating Combustion Processes with Water Injection." NACA Report 1006, 1951.

82. Wilcox, J. D. and June, R. K. "Apparatus for Study of the Breakup of Liquid Drops by High Velocity Airstreams." U. S. Army Chemical Warfare Laboratories, CWL Special Publication 1-4 May 1958.

83. Wolfson, B. T. and Dunn, R. G. "Thermodynamic Properties of Selected Species Containing Carbon, Hydrogen, Oxygen, Helium, and Argon." ARL-62-390, August 1962.

APPENDIXES

I. ILLUSTRATIONS
II. TABLES
III. PROCEDURE FOR SOLUTION OF EQUATIONS
IV. SOLUTIONS OF THE MOMENTUM EQUATIONS

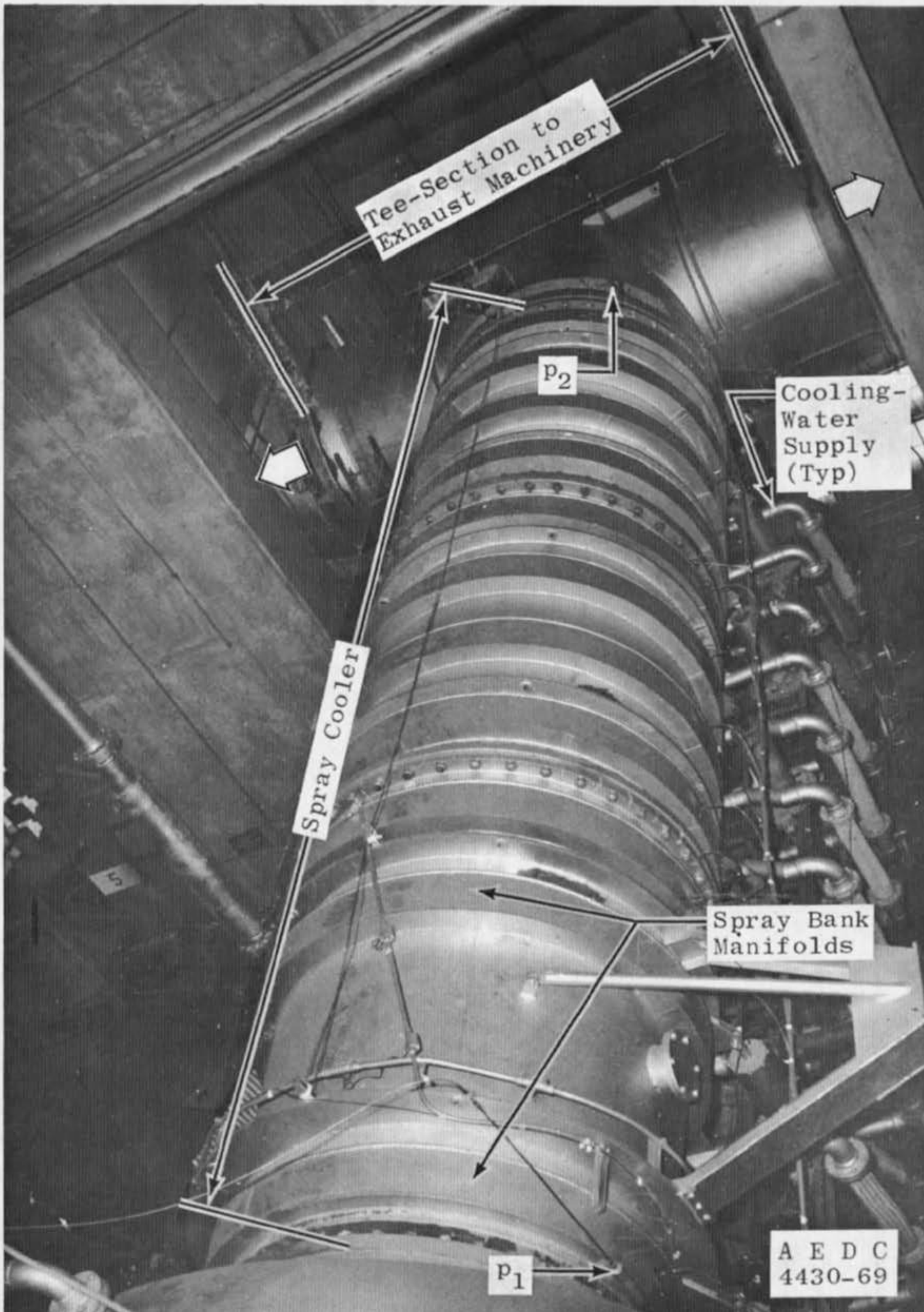

Fig. 1 Exhaust Gas Cooler in Propulsion Development Test Cell (T-1)

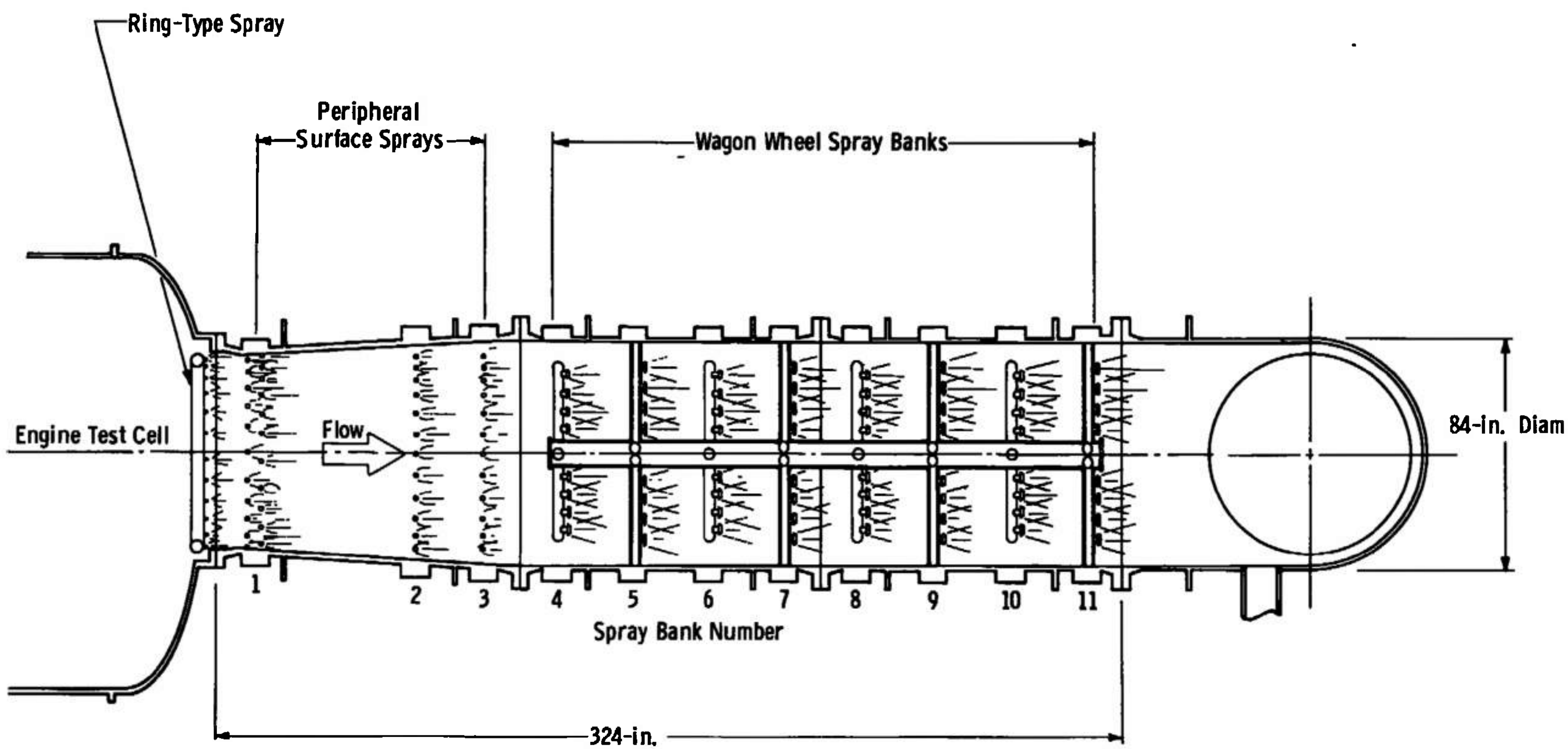

a. Section View Showing Internal Configuration
Fig. 2 Arrangement of Spray Banks in T-1 Cooler

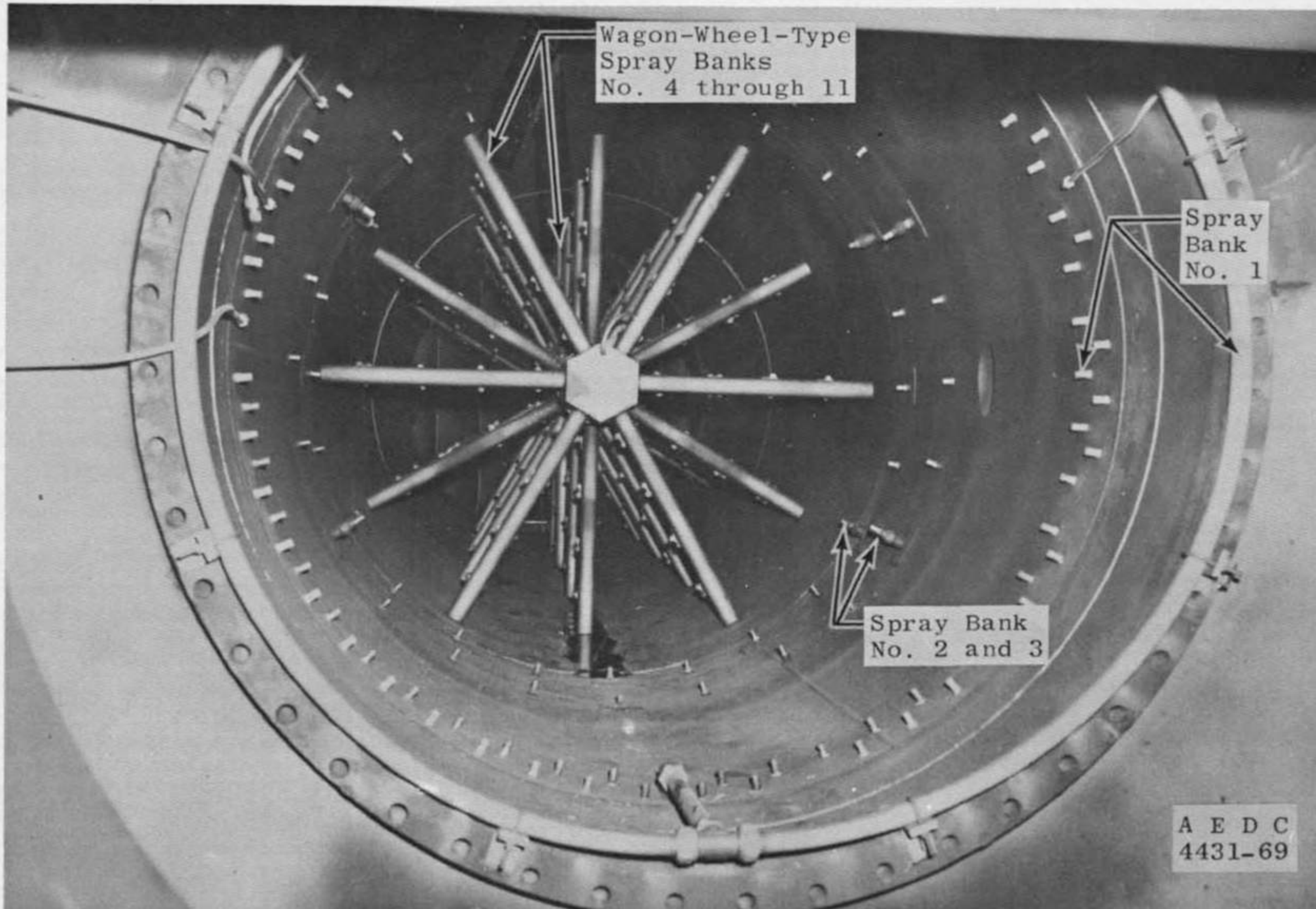

b. Internal View Showing Bank Configuration
Fig. 2 Continued

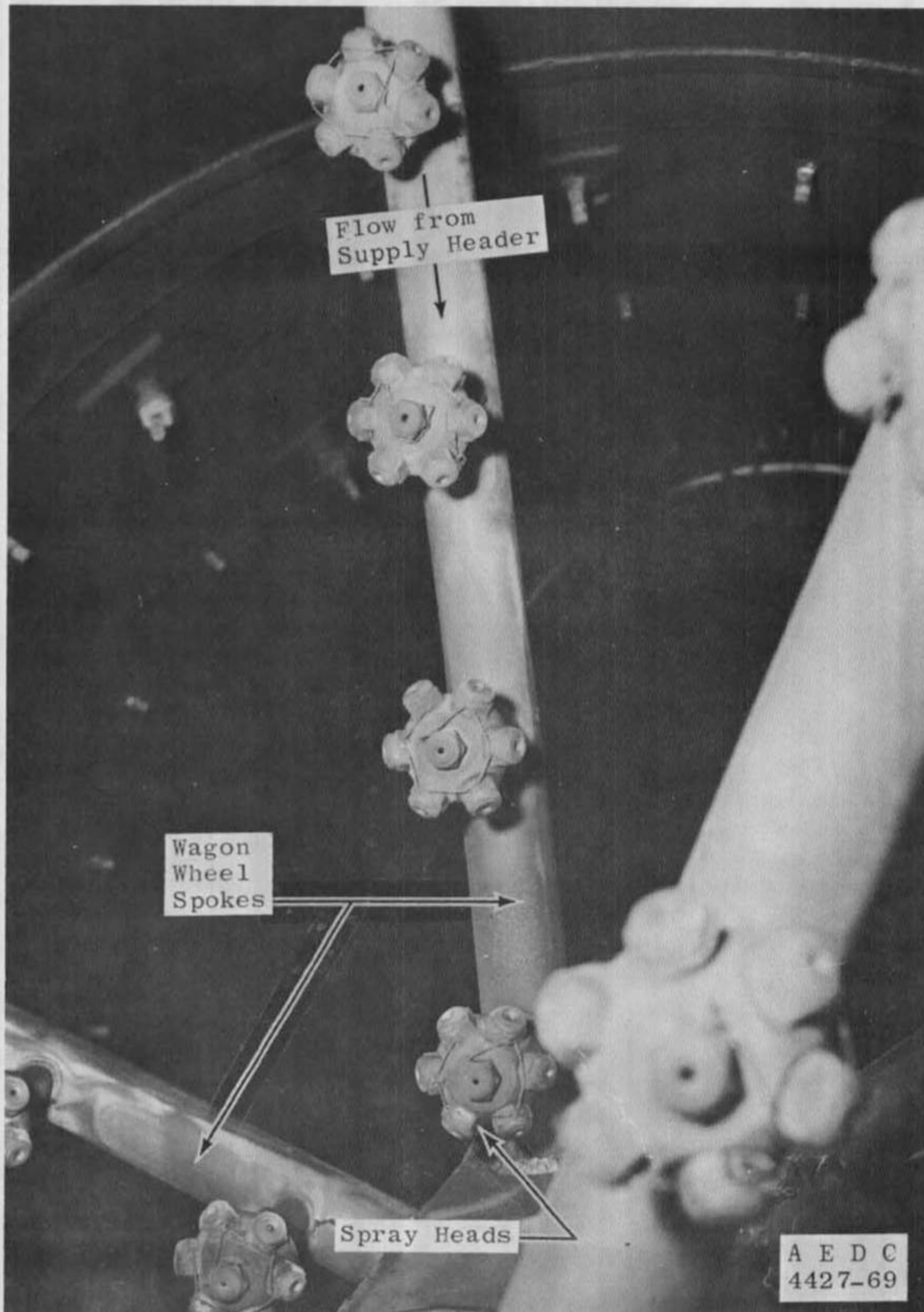

c. Multinozzle Spray Heads, View Looking Upstream (Banks No. 4 through 11)
Fig. 2 Concluded

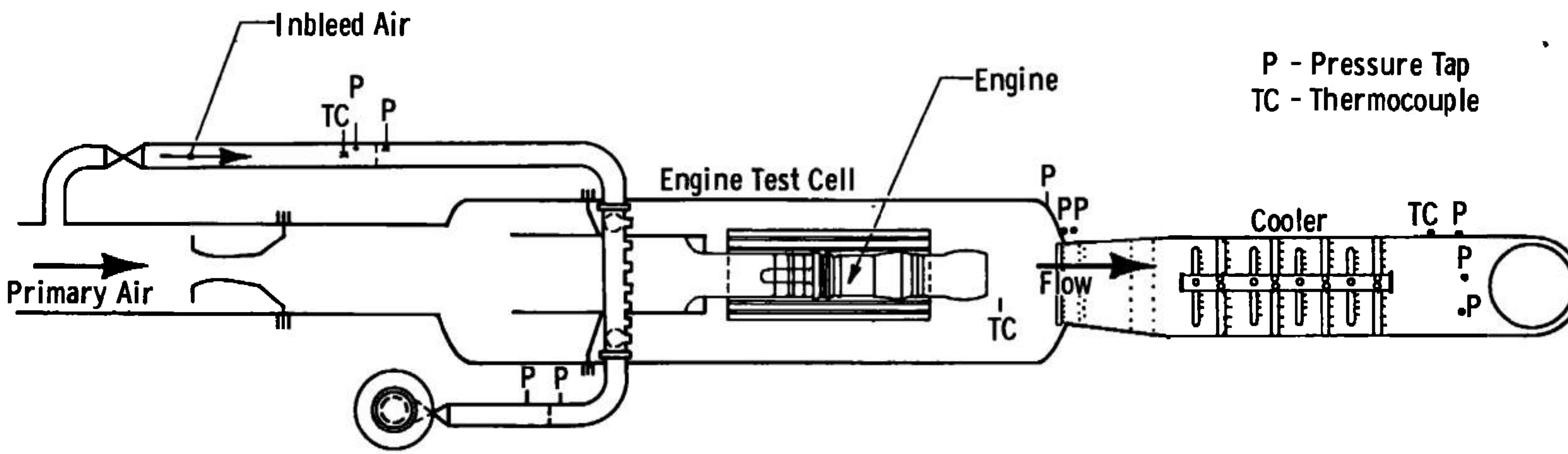

Fig. 3 System Schematic Showing Instrumentation Location

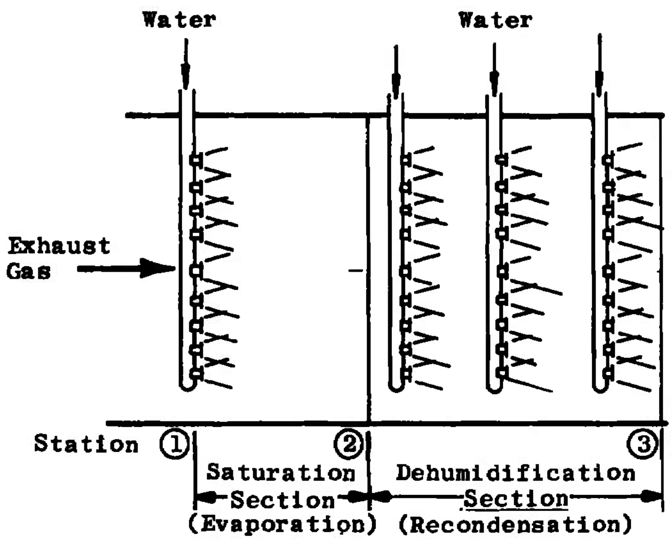

Fig. 4 Schematic Diagram of Cooler

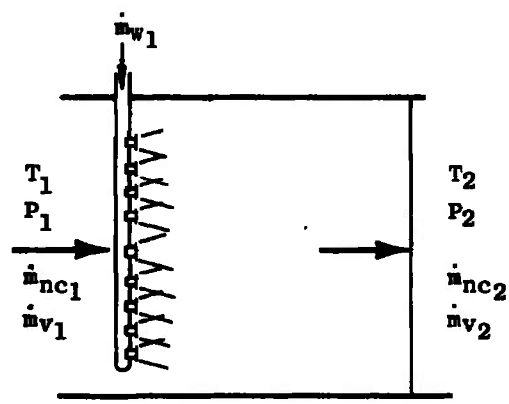

Fig. 5 Analytical Model of Evaporative Cooler (Schematic)

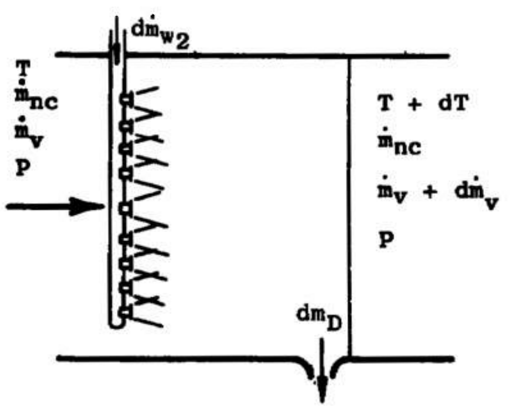

Fig. 6 Analytical Model Element of Dehumidification Cooler (Schematic)

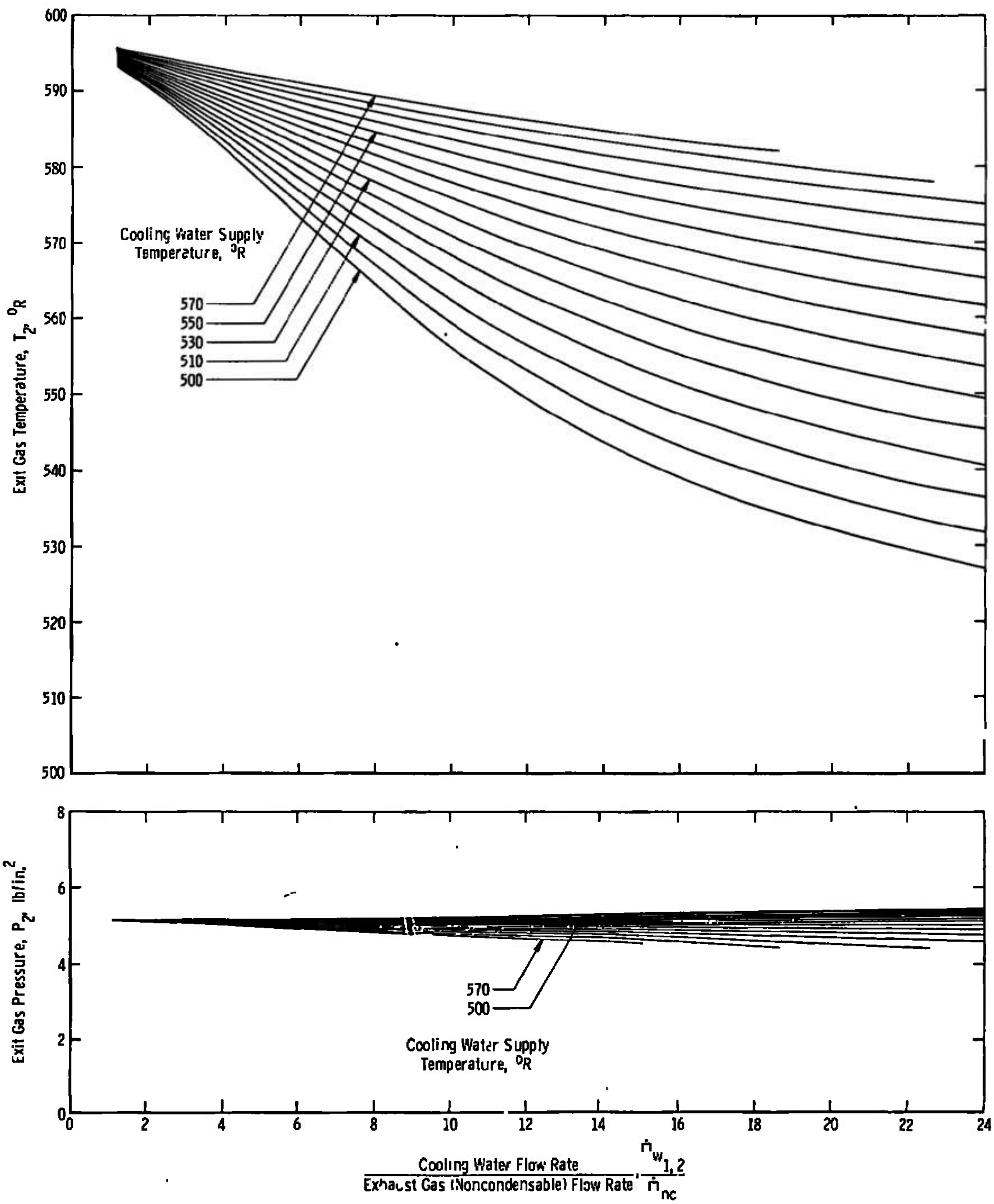

Fig. 7 Effect of Cooling Water Temperature on Exhaust Gas Temperature and Pressure (Case I)

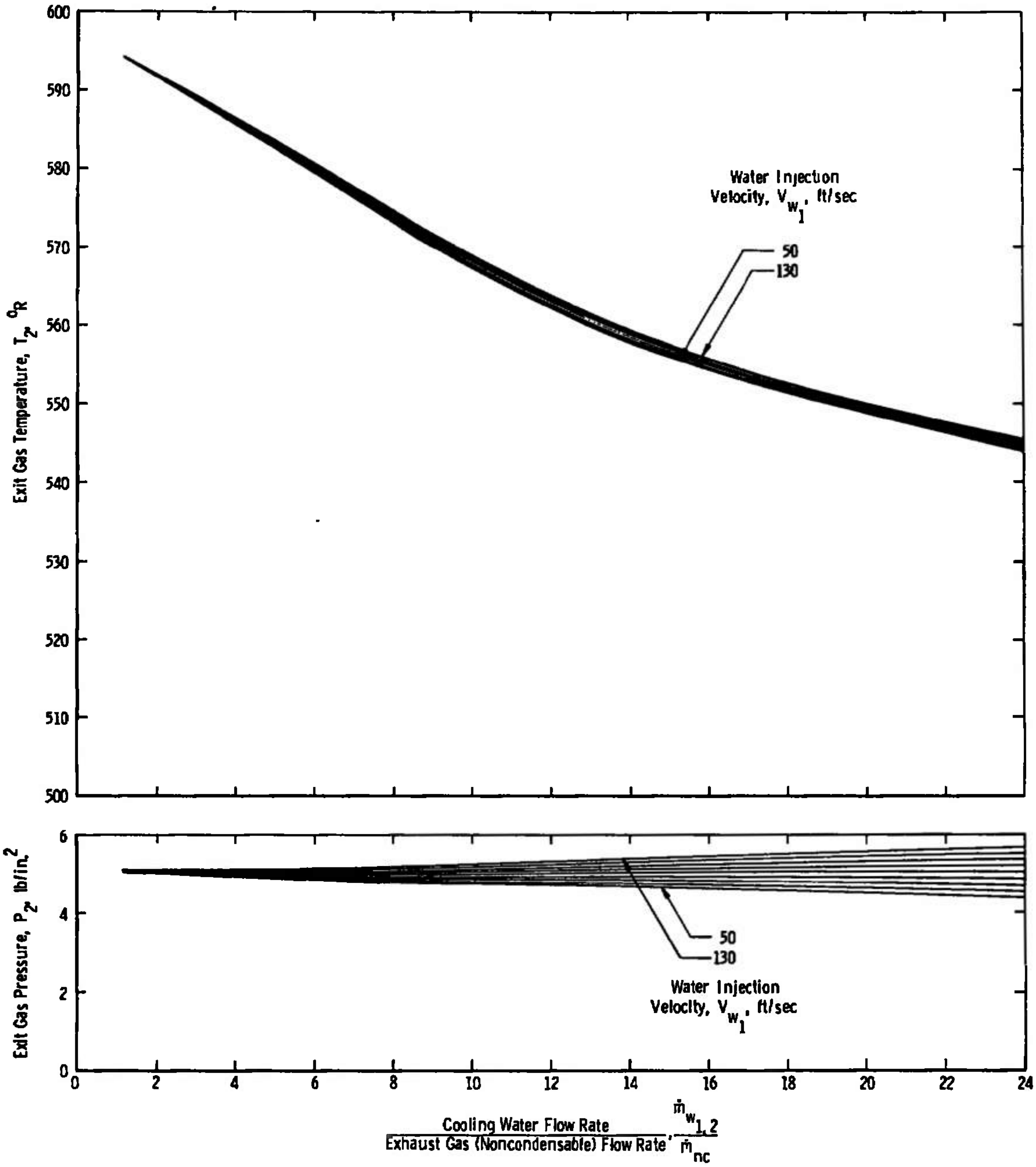

Fig. 8 Influence of Cooling Water Injection Velocity on Exhaust Gas Temperature and Pressure (Case II)

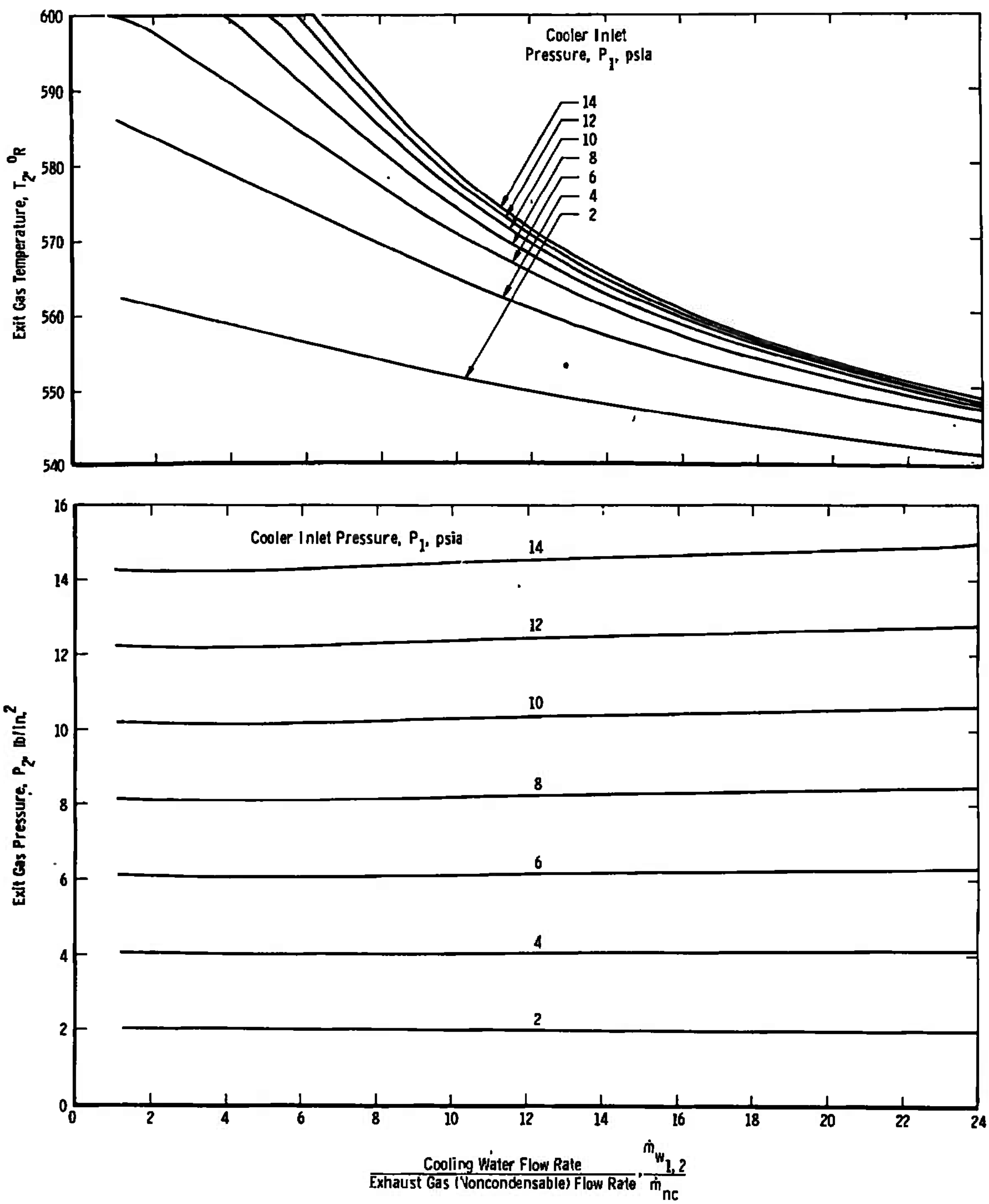

Fig. 9 Change in Exhaust Gas Temperature and Pressure Caused by Varying the Cooler Inlet Pressure (Case III)

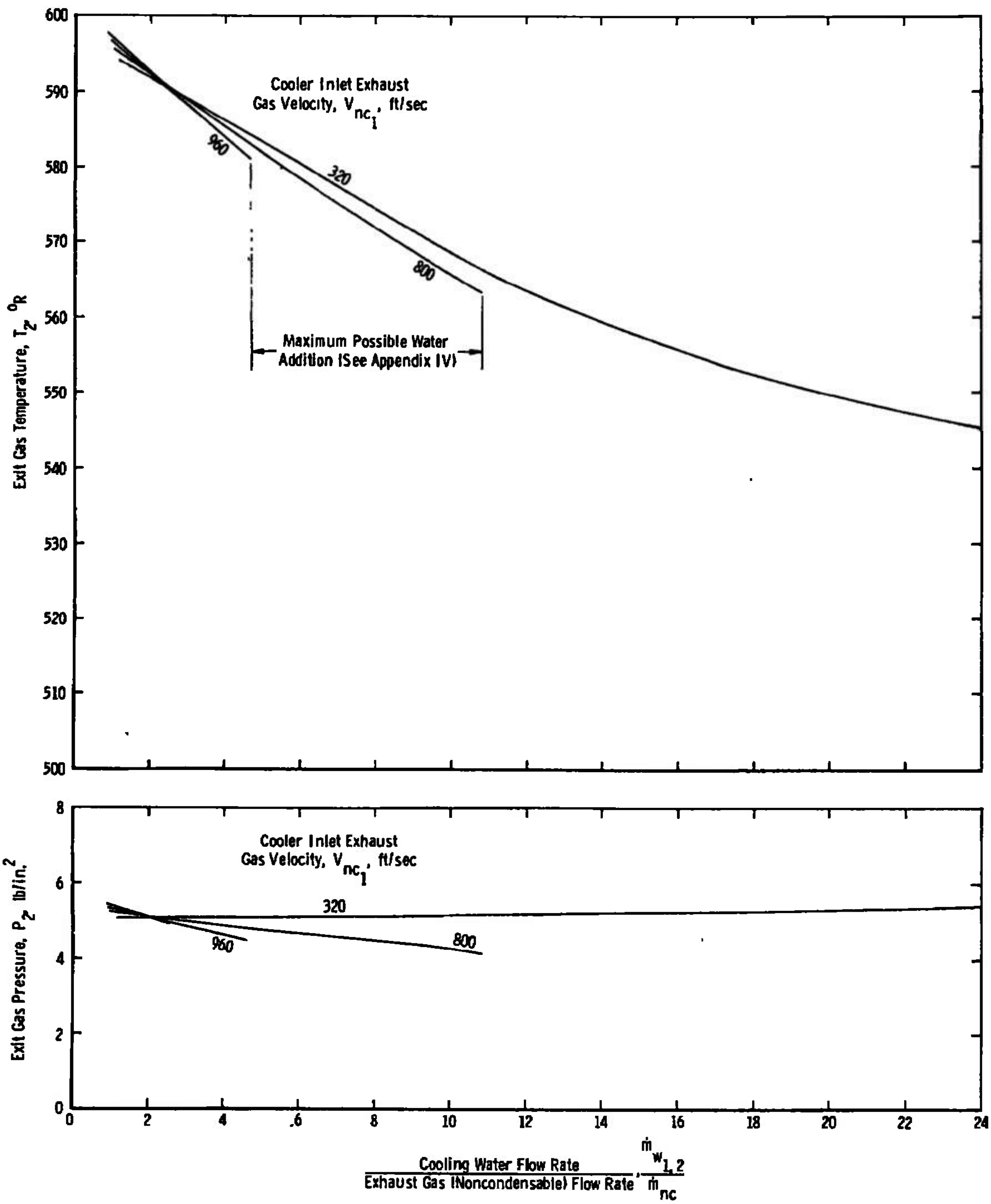

Fig. 10 Influence of Inlet Gas Velocity on the Exhaust Gas Temperature and Pressure (Case IV)

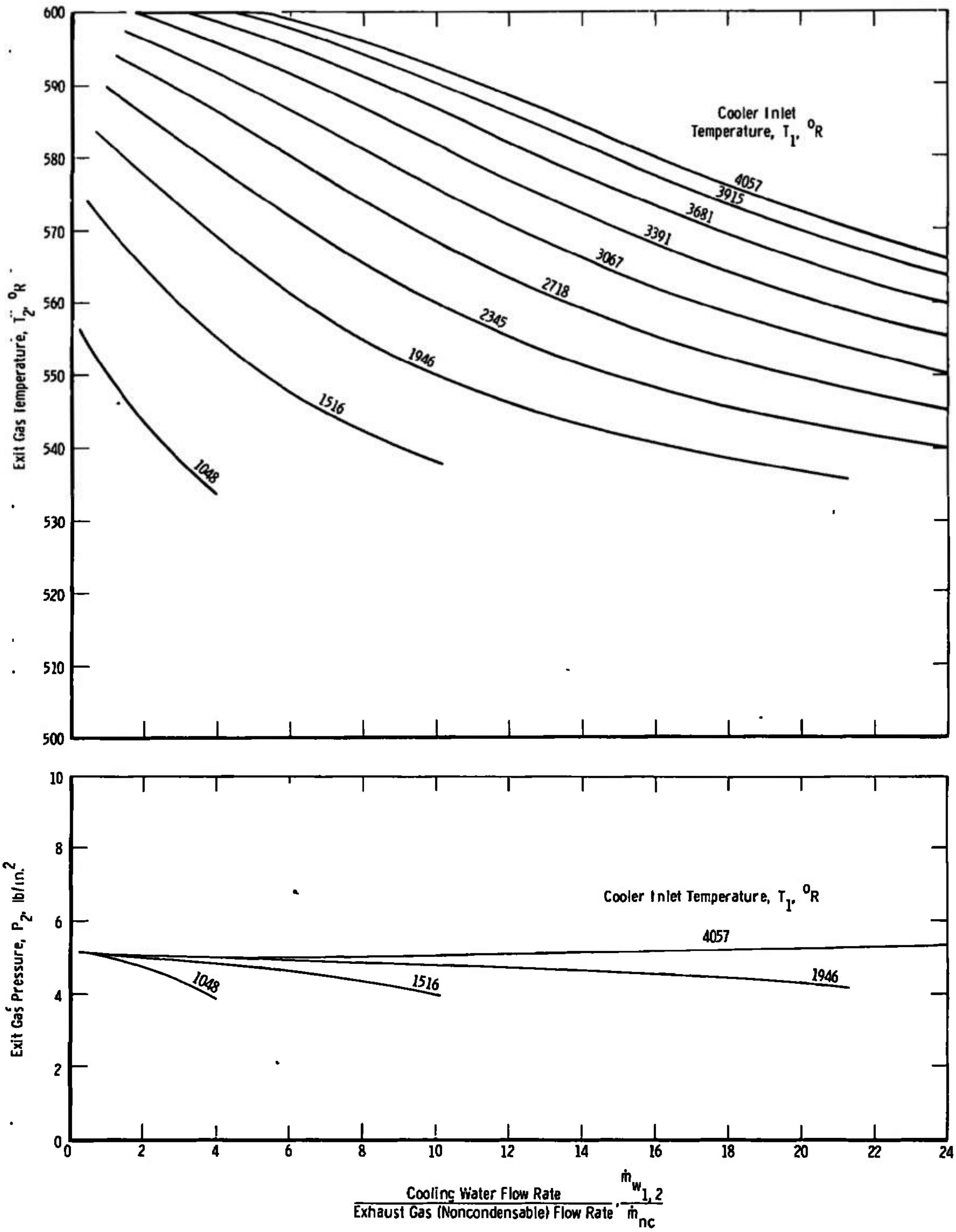

Fig. 11 Effect of Inlet Gas Temperature Change on the Exhaust Gas Temperature and Pressure (Case V)

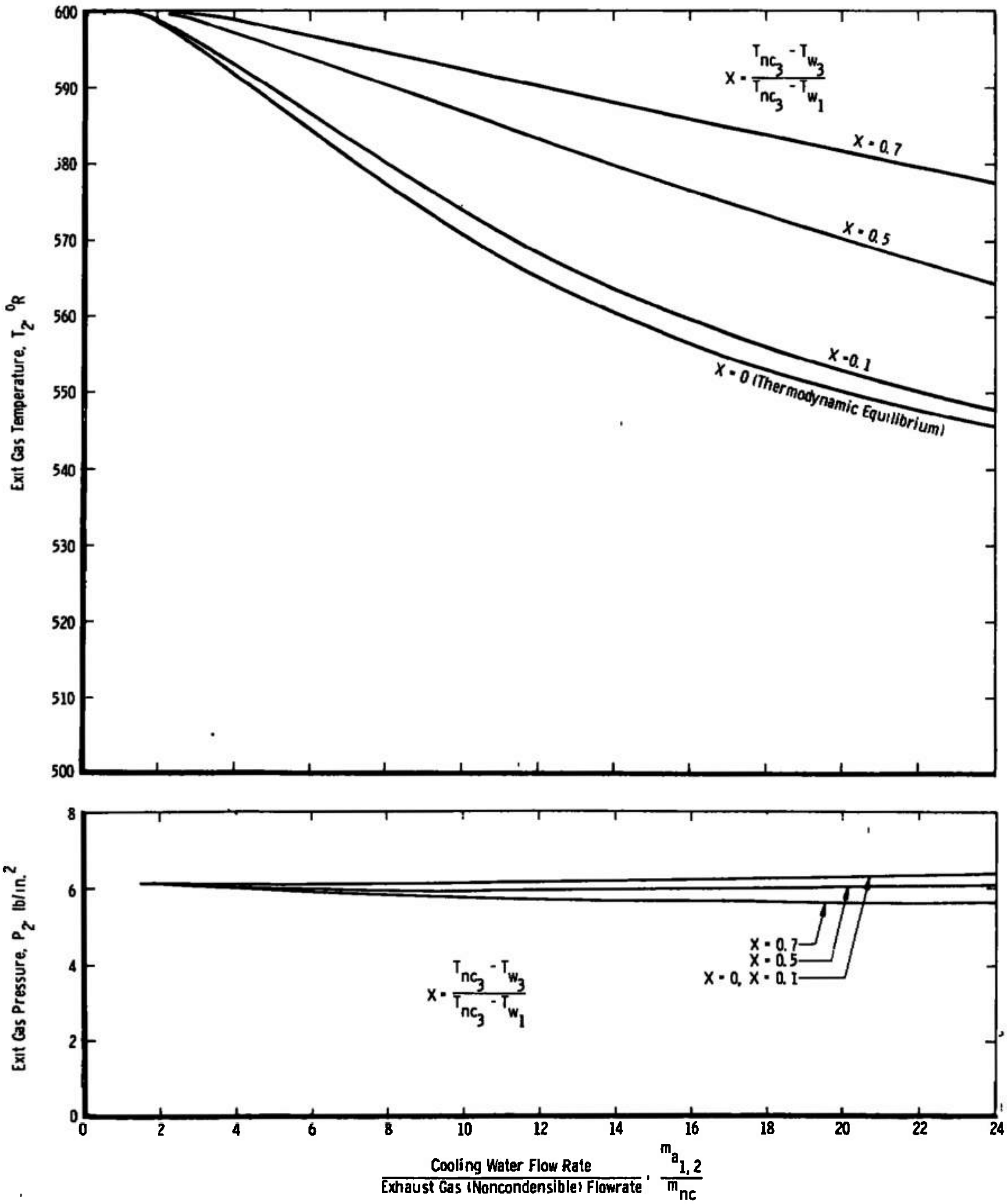

Fig. 12 Influence of Thermodynamic Nonequilibrium on the Exhaust Gas Exit Temperature and Pressure

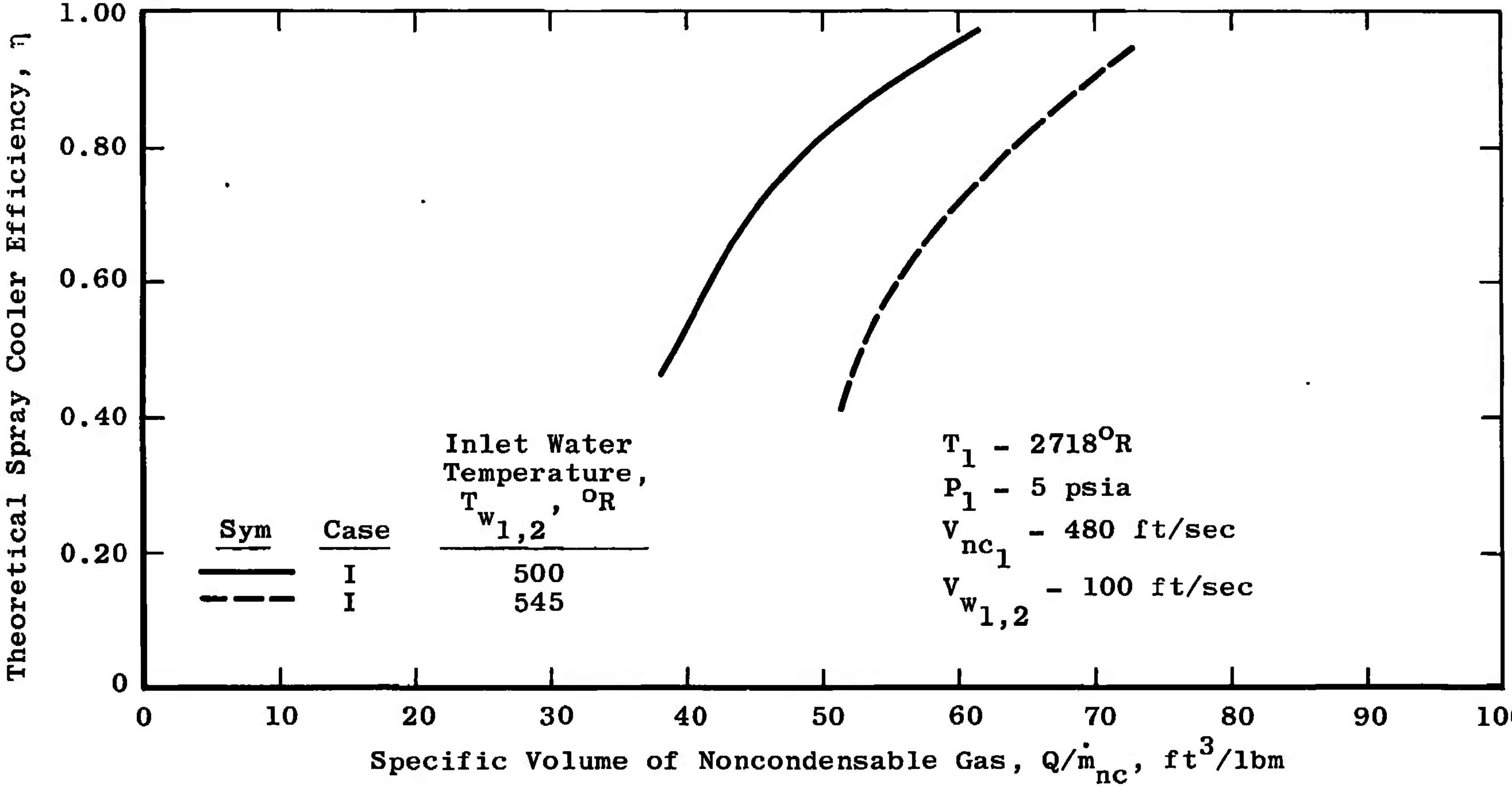

a. Effects of Changing the Cooling Water Temperature
Fig. 13 Influence of Cooling Water on Efficiency

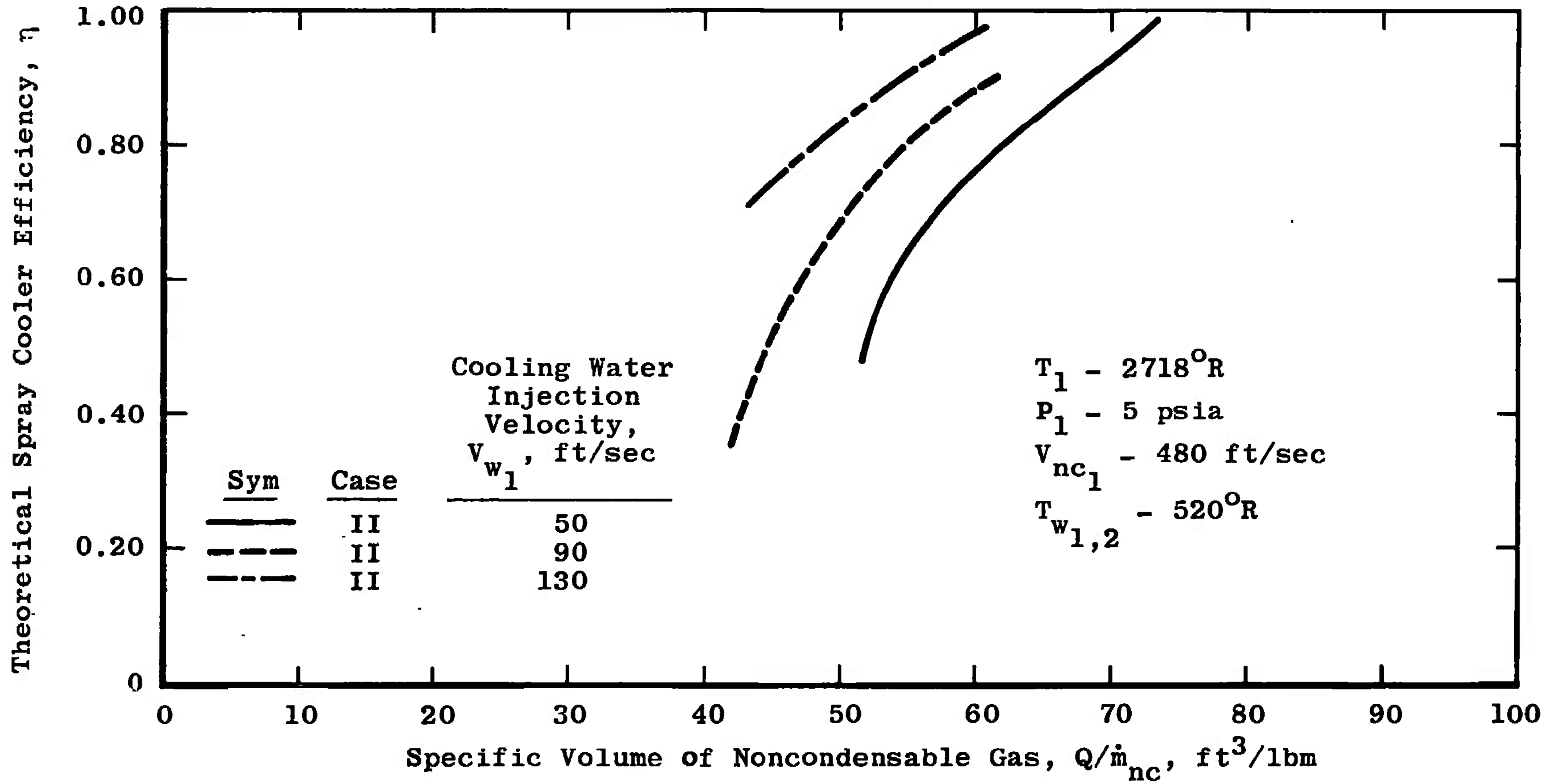

b. Effects of Changing the Cooling Water Injection Velocity
Fig. 13 Continued

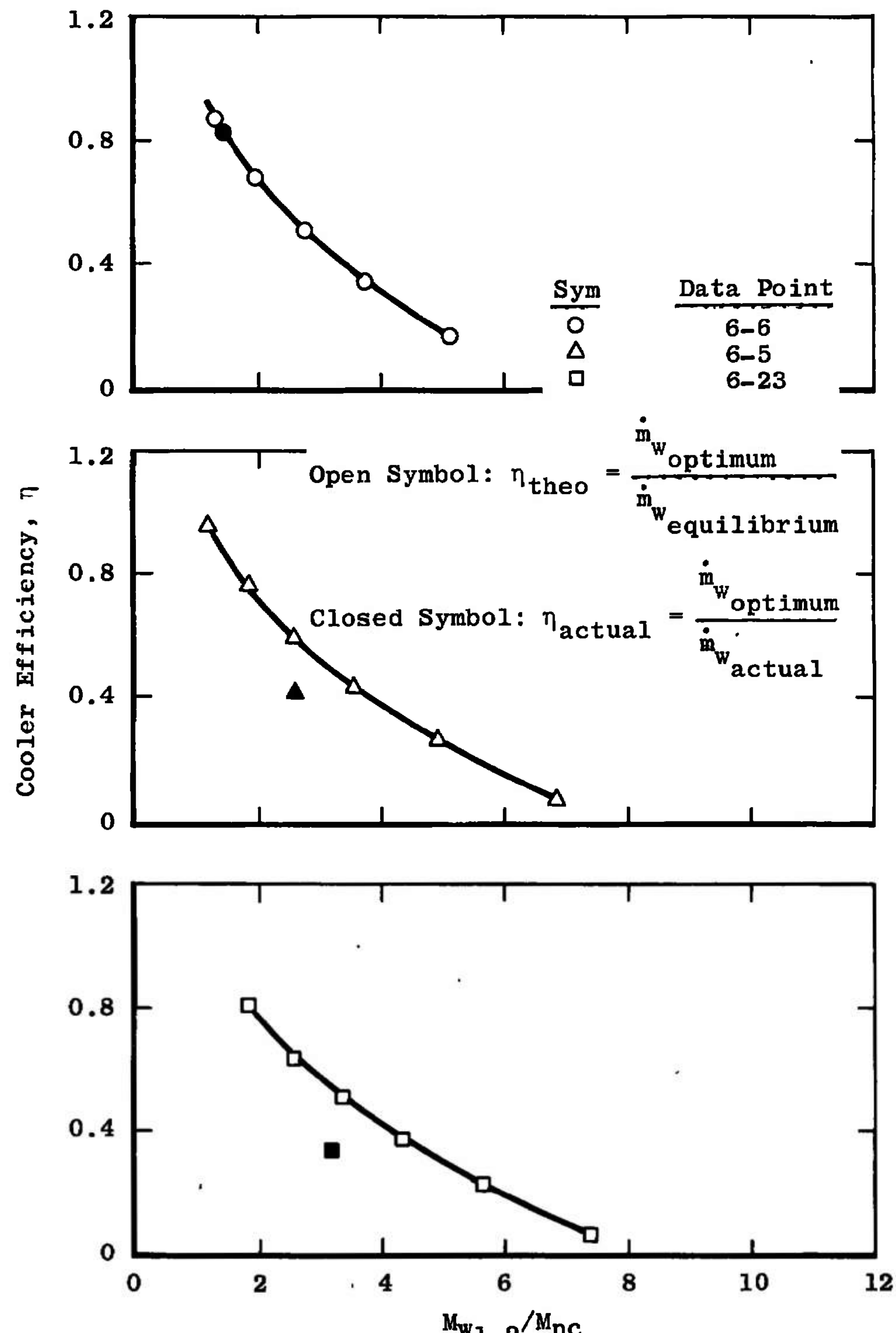

c. Comparison of $\eta_{theoretical}$ and η_{actual} as a Function of the Cooling Water Flow Rate

Fig. 13 Continued

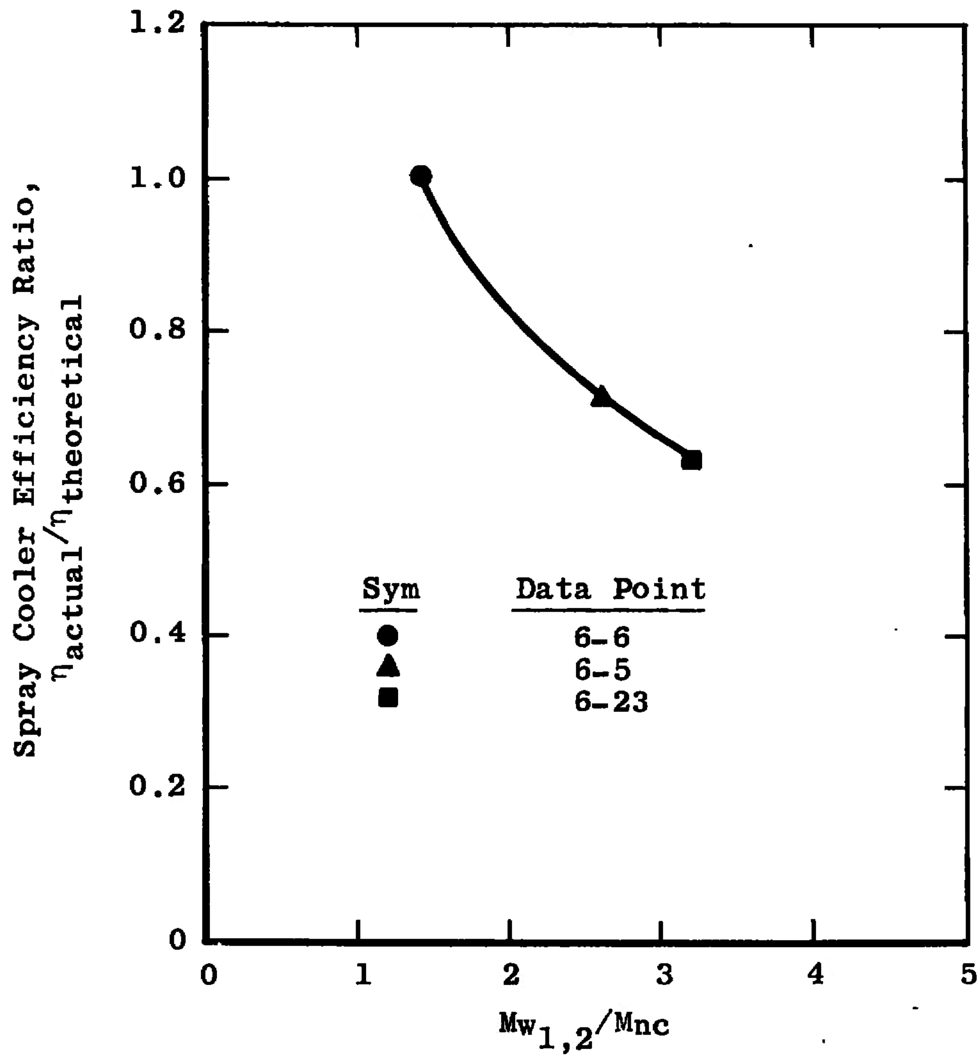

d. Effect of Varying the Mass Flow Rate Ratio on the Degree of Theoretical Efficiency Achieved
Fig. 13 Concluded

TABLE I
PARAMETRIC GRID OF INLET CONDITIONS (COMPUTER CASES)

Cases	Parameters					Remarks
	T_1 °R	p_1 psia	V_{nc_1} ft/sec	$T_{w_{1,2}}$ °R	$V_{w_{1,2}}$ ft/sec	
I	2718	5	480	500 to 580	100	$T_{w_{1,2}}$ was varied in 5-deg increments
II	2718	5	480	520	50 to 130	$V_{w_{1,2}}$ was varied in 10-ft/sec increments
III	2718	2 to 14	480	520	100	p_1 was varied in 2-psi increments
IV	2718	5	320 to 2130	520	100	V_{nc_1} was varied in nonuniform increments
V	1048 to 4057	5	480	520	100	T_1 was varied in nonuniform increments

TABLE II
KINETIC EQUILIBRIUM INFLUENCE, VALUE OF MOMENTUM EQUATION TERMS

$\frac{\dot{m}_{w_{1+2}}}{\dot{m}_{nc}}$	$\frac{P_1 A_1}{\dot{m}_{nc}}$	$\left(\frac{\dot{m}_{v_1}}{\dot{m}_{nc}} + 1\right)\frac{V_{nc_1}}{g}$	$\frac{\dot{m}_{w_{1+2}}}{\dot{m}_{nc}} \frac{V_{w_1}}{g}$	$\frac{P_3 A_3}{\dot{m}_{nc}}$	$\left(\frac{\dot{m}_{v_3}}{\dot{m}_{nc}} + 1\right)\frac{V_{nc_3}}{g}$	$\frac{\dot{m}_{w_3}}{\dot{m}_{nc}} \frac{V_{nc_3}}{g}$	$\left(\frac{\dot{m}_{w_3}}{\dot{m}_{nc}} \frac{V_{nc_3}}{g} \Big/ \text{Total Momentum}\right) \times 100\%$
1.15	316.4	15.5	3.5	323.0	9.17	3.61	1.1%
5.13	316.4	15.5	15.9	319.8	6.00	22.05	6.3%
10.46	316.4	15.5	32.4	322.8	4.16	37.21	10.2%
23.41	316.4	15.5	72.6	332.1	3.15	69.18	17.1%

TABLE III
SPRAY COOLER CONDITIONS USED FOR CALCULATING EFFICIENCIES

Run No.	P_1 psia	T_1 °R	V_{nc_1} ft/sec	T_{w_1} °R	V_{w_1} ft/sec	$\dot{m}_{w_{1+2}}/\dot{m}_{nc}$ Actual
6-6	5.1	1096	368	512	70	1.42
6-5	5.1	1096	360	512	80	2.60
6-23	5.1	1096	374	512	100	3.16

APPENDIX III
PROCEDURE FOR SOLUTION OF EQUATIONS

I. Solution of Equilibrium Equations

The procedure for determining exit conditions by solving Eqs. (7) or (11) and (17) involves two separate steps as follows:

For that part of the process leading to saturation:

1. Let $P_2 = P_1$.
2. Assume a T_2.
3. Calculate a new temperature ($T2_{new}$) using Eq. (7), Eqs. (9) and (10) in which Dalton's law is used to eliminate P_{nc}, and the partial pressure-temperature relationship.
4. Compare $T2_{new}$ with the assumed temperature in step 2. If their difference is within tolerance, proceed to step 5; otherwise let $T_2 = T2_{new}$, and go back to step 3.
5. Calculate a new pressure ($P2_{new}$) using Eq. (17).
6. Compare $P2_{new}$ with P_2 in step 1. If their difference is within tolerance, P_2 is the saturation pressure, and T_2 is the saturation temperature; otherwise let $P_2 = P2_{new}$, $T_2 = T2_{new}$, and go back to step 3.

For that part of the process beyond saturation (dehumidification):

1. Let $T_3 = T_{saturation} - \Delta T$.where ΔT is some small temperature increment on the order of one degree.
2. Let $P_3 = P_s$.
3. Calculate a new pressure ($P3_{new}$) using the partial pressure-temperature relationship, Eqs. (9), (11), and (17).
4. Compare $P3_{new}$ with the pressure (P_3) in step 2. If their difference is within tolerance, the equations are satisfied at the assumed temperature (T_2). Go to step 5. Otherwise let $P_3 = \dfrac{P_3 + P3_{new}}{2}$, and go to step 3.

5. Let $T_3 = T_3 - \Delta T$. Go to step 2.

The dehumidification procedure is allowed to continue until $T_3 = T_{w2}$.

II. Solution of Efficiency Equations

The procedure for solution of Eq. (27) for the saturation case is as follows:

1. Determine P_{v3}, a known function of T, at an assumed T_3.
2. Calculate $P_{v3_{new}}$ from Eq. (28).
3. Determine $T_{3_{new}}$, a known function of P_v, at $P_{v3_{new}}$.
4. Compare $P_{v3_{new}}$ with P_{v3}. If their difference is within tolerance, let $P_{v_{3new}} = P_{v_3}$, and proceed to step 5; otherwise let $P_{v_3} = \dfrac{P_{v_3} + P_{v_{3new}}}{2}$ and $T_3 = T_{3_{new}}$, and go back to step 2.
5. Calculate the water required for stauration using Eq. (27).

For the dehumidification case, the solution of Eq. (38) is required. The procedure for solving this equation is based on a Gaussian integration technique. The term (F) is the ratio of the mass flow of the water injected into the dehumidification cooler element to the mass flow of noncondensable gases, $F = \dot{m}_{w2}/\dot{m}_{nc}$. To determine the total mass flow ratio of the entire cooler, the water injected into the saturation section $(\dot{m}_{w1_{evap}}/\dot{m}_{nc})$ can be added to F. This will give the ideal mass flow ratio $(\dot{m}_{w_{ideal}}/\dot{m}_{nc})$. From this can be calculated the value of total water required for the entire cooler for the idealized case $(\dot{m}_{w_{ideal}})$.

APPENDIX IV
SOLUTIONS OF THE MOMENTUM EQUATION

The original development of the momentum equation in Section III led to the solution of the exit pressure (P_3) from an equation of the quadratic type:

$$P_3 = \frac{-b + \sqrt{b^2 - 4ac}}{2a}$$

where a, b, and c have previously been defined. The possibility of the quantity $b^2 - 4ac$ becoming negative and giving an exit pressure in terms of a complex number is immediately recognized. The question becomes (1) will this happen during numerical solution, and (2) if it does, is there a physical explanation?

For certain cooler inlet conditions, $b^2 - 4ac$ does become negative during the numerical solution. Correspondingly, there is a minimum value of T_2 and a maximum value of $\dot{m}_{w1,2}/\dot{m}_{nc}$, say $(\dot{m}_{w1,2}/\dot{m}_{nc})_{max}$, for which a solution can be obtained to the momentum equation. A physical interpretation of this behavior is that it is impossible for equilibrium to exist at the exit of the cooler when the value of the water added to the cooler exceeds $(\dot{m}_{w1,2}/\dot{m}_{nc})_{max}$. If the cooler is operating with equilibrium at the exit and the rate of cooling water injection equals to $(\dot{m}_{w1,2}/\dot{m}_{nc})_{max}$ and the rate of cooling water injection is increased, the gas phase will choke at the cooler exit, and thermodynamic and kinetic equilibrium cannot exist at the exit. Any further increase in water injection rate must cause an adjustment in the initial conditions. The analysis indicates a sudden choking condition. That is, the gas phase Mach number at the cooler exit would suddenly jump from some subsonic valve to unity with the addition of a differential amount of water. However, in an actual cooler which has finite length, sudden choking would not be expected to occur because of nonequilibrium effects. Also, the value of $\dot{m}_{w1,2}/\dot{m}_{nc}$ at which choking would occur in an actual cooler would be somewhat higher than $(\dot{m}_{w1,2}/\dot{m}_{nc})_{max}$.

DOCUMENT CONTROL DATA - R & D

(Security classification of title, body of abstract and indexing annotation must be entered when the overall report is classified)

1. ORIGINATING ACTIVITY *(Corporate author)* Arnold Engineering Development Center, ARO, Inc., Operating Contractor, Arnold Air Force Station, Tennessee 37389	2a. REPORT SECURITY CLASSIFICATION UNCLASSIFIED 2b. GROUP N/A

3 REPORT TITLE
ANALYTICAL MODEL OF AN EXHAUST GAS COOLING SYSTEM EMPLOYING LIQUID INJECTION

4 DESCRIPTIVE NOTES *(Type of report and inclusive dates)*
Final Report

5 AUTHOR(S) *(First name, middle initial, last name)*
J. M. Pelton and C. E. Willbanks, ARO, Inc.

6 REPORT DATE	7a. TOTAL NO OF PAGES	7b. NO. OF REFS
June 1971	55	83

8a. CONTRACT OR GRANT NO. F40600-71-C-0002 Program Element 6540223F	9a. ORIGINATOR'S REPORT NUMBER(S) AEDC-TR-71-60 9b. OTHER REPORT NO(S) *(Any other numbers that may be assigned this report)* ARO-ETF-TR-70-306

10 DISTRIBUTION STATEMENT
Approved for public release; distribution unlimited.

11 SUPPLEMENTARY NOTES	12. SPONSORING MILITARY ACTIVITY
Available in DDC	Arnold Engineering Development Center (XOO), Arnold Air Force Station, Tennessee 37389

13. ABSTRACT

An analysis was undertaken to better understand the phenomena occurring in spray coolers and to develop a mathematical model for comparison with experimental data from an operating unit. The physical characteristics of an operational exhaust gas spray cooler and the instrumentation systems are described. A mathematical model of a spray cooler was developed by assuming kinetic and thermodynamic equilibrium and one-dimensional flow. A mathematical model of a hypothetical, optimum cooler is included in order to have a basis for defining cooler efficiency. The equations were programmed for numerical solution on a digital computer, and several trial case runs are presented. Experimental measurements are compared with the efficiencies predicted by the mathematical models.

14. KEY WORDS	LINK A		LINK B		LINK C	
	ROLE	WT	ROLE	WT	ROLE	WT
computer programming						
mathematical analysis						
mathematical model						
one-dimensional flow						
exhaust gases						
spray nozzles						
coolers						
cooling with liquids						
kinetic theory						
thermodynamic properties						
test facilities						

AFSC
Arnold AFS Tenn